Prédiction de la réponse thérapeutique précoce par TEP au 18FDG dans le cancer du sein HER2+ : Approche conventionnelle et analyse texturale en situation néoadjuvante

Marion Chanchou

UFR DE MÉDECINE
ET DES PROFESSIONS PARAMÉDICALES
Université Clermont Auvergne

N°

Année 2019

UNIVERSITÉ CLERMONT AUVERGNE
UFR DE MÉDECINE ET DES PROFESSIONS PARAMÉDICALES

THÈSE D'EXERCICE
pour le
DIPLÔME D'ÉTAT DE DOCTEUR EN MÉDECINE
par

CHANCHOU Marion

Présentée et soutenue publiquement le 03 septembre 2019

Prédiction de la réponse thérapeutique précoce par TEP au ^{18}FDG dans le cancer du sein HER2+ : Approche conventionnelle et analyse texturale en situation néoadjuvante.

Directeur de thèse : Monsieur CACHIN Florent, Professeur, Centre de Lutte contre le Cancer Jean Perrin (Service de Médecine Nucléaire)

Président du jury : Madame PENAULT-LLORCA Frédérique, Professeur, UFR de Médecine et des professions paramédicales de Clermont-Ferrand.

Membres du jury :
Madame PENAULT-LLORCA Frédérique, Professeur, UFR de Médecine et des professions paramédicales de Clermont-Ferrand.
Monsieur CACHIN Florent, Professeur, UFR de Médecine et des Professions paramédicales de Clermont-Ferrand
Monsieur DURANDO Xavier, Professeur, UFR de Médecine et des professions paramédicales de Clermont-Ferrand.
Madame ORLHAC Fanny, PhD, Chercheure post-doctorante, Equipe-projet Epione, Inria, Sophia-Antipolis.

UFR DE MÉDECINE
ET DES PROFESSIONS PARAMÉDICALES
Université Clermont Auvergne

N°

Année 2019

UNIVERSITÉ CLERMONT AUVERGNE
UFR DE MÉDECINE ET DES PROFESSIONS PARAMÉDICALES

THÈSE D'EXERCICE
pour le
DIPLÔME D'ÉTAT DE DOCTEUR EN MÉDECINE
par

CHANCHOU Marion

Présentée et soutenue publiquement le 03 septembre 2019

Prédiction de la réponse thérapeutique précoce par TEP au ^{18}FDG dans le cancer du sein HER2+ : Approche conventionnelle et analyse texturale en situation néoadjuvante.

Directeur de thèse : Monsieur CACHIN Florent, Professeur, Centre de Lutte contre le Cancer Jean Perrin (Service de Médecine Nucléaire)

Président du jury : Madame PENAULT-LLORCA Frédérique, Professeur, UFR de Médecine et des professions paramédicales de Clermont-Ferrand.

Membres du jury :
Madame PENAULT-LLORCA Frédérique, Professeur, UFR de Médecine et des professions paramédicales de Clermont-Ferrand.
Monsieur CACHIN Florent, Professeur, UFR de Médecine et des Professions paramédicales de Clermont-Ferrand
Monsieur DURANDO Xavier, Professeur, UFR de Médecine et des professions paramédicales de Clermont-Ferrand.
Madame ORLHAC Fanny, PhD, Chercheure post-doctorante, Equipe-projet Epione, Inria, Sophia-Antipolis.

UNIVERSITE CLERMONT AUVERGNE

PRESIDENTS HONORAIRES UNIVERSITE D'AUVERGNE : JOYON Louis - DOLY Michel - TURPIN Dominique - VEYRE Annie - DULBECCO Philippe - ESCHALIER Alain
PRESIDENTS HONORAIRES UNIVERSITE BLAISE PASCAL : CABANES Pierre - FONTAINE Jacques -BOUTIN Christian - MONTEIL Jean-Marc - ODOUARD Albert - LAVIGNOTTE Nadine
PRESIDENT DE L'UNIVERSITE et PRESIDENT DU CONSEIL ACADEMIQUE PLENIER : BERNARD Mathias
PRESIDENT DU CONSEIL ACADEMIQUE RESTREINT : DEQUIEDT Vianney
VICE-PRESIDENT DU CONSEIL D'ADMINISTRATION : WILLIAMS Benjamin
VICE-PRESIDENT DE LA COMMISSION DE LA RECHERCHE : HENRARD Pierre
VICE PRESIDENTE DE LA COMMISSION DE LA FORMATION ET DE LA VIE UNIVERSITAIRE : PEYRARD Françoise
DIRECTEUR GENERAL DES SERVICES : PAQUIS François

UFR DE MEDECINE ET DES PROFESSIONS PARAMEDICALES

DOYENS HONORAIRES : DETEIX Patrice - CHAZAL Jean
DOYEN : CLAVELOU Pierre
RESPONSABLE ADMINISTRATIVE : ROBERT Gaëlle

LISTE DU PERSONNEL ENSEIGNANT

PROFESSEURS HONORAIRES :
MM. BACIN Franck - BEGUE René-Jean - BOUCHER Daniel - BOURGES Michel - BUSSIERE Jean-Louis - CANO Noël - CASSAGNES Jean - CATILINA Pierre - CHABANNES Jacques – CHAZAL Jean - CHIPPONI Jacques - CHOLLET Philippe - COUDERT Jean - DASTUGUE Bernard - DEMEOCQ François - DE RIBEROLLES Charles - ESCANDE Georges - Mme FONCK Yvette - MM. GENTOU Claude - GLANDDIER Gérard - Mmes GLANDDIER Phyllis - LAVARENNE Jeanine - MM. LAVERAN Henri - LEVAI Jean-Paul - MAGE Gérard - MALPUECH Georges - MARCHEIX Jean-Claude - MICHEL Jean-Luc - MOLINA Claude - MONDIE Jean-Michel - PERI Georges - PETIT Georges - PHILIPPE Pierre - PLAGNE Robert - PLANCHE Roger - PONSONNAILLE Jean - RAYNAUD Elie - REY Michel - Mme RIGAL Danièle - MM. ROZAN Raymond - SCHOEFFLER Pierre - SIROT Jacques - SOUTEYRAND Pierre - TANGUY Alain - TERVER Sylvain - THIEBLOT Philippe - TOURNILHAC Michel - VANNEUVILLE Guy - VIALLET Jean-François - Mle VEYRE Annie

PROFESSEURS EMERITES :
MM. - BEYTOUT Jean - BOITEUX Jean-Paul - BOMMELAER Gilles - CHAMOUX Alain - DAUPLAT Jacques - DETEIX Patrice - ESCHALIER Alain - IRTHUM Bernard - JACQUETIN Bernard - KEMENY Jean-Louis – Mme LAFEUILLE Hélène – MM. LEMERY Didier - LESOURD Bruno - LUSSON Jean-René - RIBAL Jean-Pierre

PROFESSEURS DES UNIVERSITES-PRATICIENS HOSPITALIERS

PROFESSEURS DE CLASSE EXCEPTIONNELLE :
M. VAGO Philippe : Histologie-Embryologie Cytogénétique
M. AUMAITRE Olivier : Médecine Interne
M. LABBE André : Pédiatrie
M. AVAN Paul : Biophysique et Traitement de l'Image
M. DURIF Franck : Neurologie

M. BOIRE Jean-Yves : Biostatistiques, Informatique Médicale et Technologies de Communication
M. BOYER Louis : Radiologie et Imagerie Médicale option Clinique
M. POULY Jean-Luc : Gynécologie et Obstétrique
M. CANIS Michel : Gynécologie-Obstétrique
Mme PENAULT-LLORCA Frédérique : Anatomie et Cytologie Pathologiques
M. BAZIN Jean-Etienne : Anesthésiologie et Réanimation Chirurgicale
M. BIGNON Yves Jean : Cancérologie option Biologique
M. BOIRIE Yves : Nutrition Humaine
M. CLAVELOU Pierre : Neurologie
M. DUBRAY Claude : Pharmacologie Clinique
M. GILAIN Laurent : O.R.L.
M. LEMAIRE Jean-Jacques : Neurochirurgie
M. CAMILLERI Lionel : Chirurgie Thoracique et Cardio-Vasculaire
M. DAPOIGNY Michel : Gastro-Entérologie
M. LLORCA Pierre-Michel : Psychiatrie d'Adultes
M. PEZET Denis : Chirurgie Digestive
M. SOUWEINE Bertrand : Réanimation Médicale
M. BOISGARD Stéphane : Chirurgie Orthopédique et Traumatologie
M. CONSTANTIN Jean-Michel : Anesthésiologie et Réanimation Chirurgicale
Mme DUCLOS Martine : Physiologie
M. SCHMIDT Jeannot : Thérapeutique

PROFESSEURS DE 1ère CLASSE :
M. DECHELOTTE Pierre : Anatomie et Cytologie Pathologique
M. CAILLAUD Denis : Pneumo-phtisiologie
M. VERRELLE Pierre : Radiothérapie option Clinique
M. CITRON Bernard : Cardiologie et Maladies Vasculaires
M. D'INCAN Michel : Dermatologie -Vénéréologie
Mme JALENQUES Isabelle : Psychiatrie d'Adultes
Mle BARTHELEMY Isabelle : Chirurgie Maxillo-Faciale
M. GARCIER Jean-Marc : Anatomie-Radiologie et Imagerie Médicale
M. GERBAUD Laurent : Epidémiologie, Economie de la Santé et Prévention
M. SOUBRIER Martin : Rhumatologie
M. TAUVERON Igor : Endocrinologie et Maladies Métaboliques
M. MOM Thierry : Oto-Rhino-Laryngologie
M. RICHARD Ruddy : Physiologie
M. RUIVARD Marc : Médecine Interne
M. SAPIN Vincent : Biochimie et Biologie Moléculaire
M. BAY Jacques-Olivier : Cancérologie
M. BERGER Marc : Hématologie
M. COUDEYRE Emmanuel : Médecine Physique et de Réadaptation
Mme GODFRAIND Catherine : Anatomie et Cytologie Pathologiques
M. ROSSET Eugénio : Chirurgie Vasculaire
M. ABERGEL Armando : Hépatologie
M. LAURICHESSE Henri : Maladies Infectieuses et Tropicales
M. TOURNILHAC Olivier : Hématologie
M. CHIAMBARETTA Frédéric : Ophtalmologie
M. FILAIRE Marc : Anatomie – Chirurgie Thoracique et Cardio-Vasculaire
M. GALLOT Denis : Gynécologie-Obstétrique
M. GUY Laurent : Urologie
M. TRAORE Ousmane : Hygiène Hospitalière
M. ANDRE Marc : Médecine Interne

M. BONNET Richard : Bactériologie, Virologie
M. CACHIN Florent : Biophysique et Médecine Nucléaire
M. COSTES Frédéric : Physiologie
M. FUTIER Emmanuel : Anesthésiologie-Réanimation
Mme HENG Anne-Elisabeth : Néphrologie
M. MOTREFF Pascal : Cardiologie
Mme PICKERING Gisèle : Pharmacologie Clinique

PROFESSEURS DE 2ème CLASSE :
Mme CREVEAUX Isabelle : Biochimie et Biologie Moléculaire
M. FAICT Thierry : Médecine Légale et Droit de la Santé
Mme KANOLD LASTAWIECKA Justyna : Pédiatrie
M. TCHIRKOV Andréï : Cytologie et Histologie
M. CORNELIS François : Génétique
M. DESCAMPS Stéphane : Chirurgie Orthopédique et Traumatologique
M. POMEL Christophe : Cancérologie – Chirurgie Générale
M. CANAVESE Fédérico : Chirurgie Infantile
M. LESENS Olivier : Maladies Infectieuses et Tropicales
M. RABISCHONG Benoît : Gynécologie Obstétrique
M. AUTHIER Nicolas : Pharmacologie Médicale
M. BROUSSE Georges : Psychiatrie Adultes/Addictologie
M. BUC Emmanuel : Chirurgie Digestive
M. CHABROT Pascal : Radiologie et Imagerie Médicale
M. LAUTRETTE Alexandre : Néphrologie Réanimation Médicale
M. AZARNOUSH Kasra : Chirurgie Thoracique et Cardiovasculaire
Mme BRUGNON Florence : Biologie et Médecine du Développement et de la Reproduction
Mme HENQUELL Cécile : Bactériologie Virologie
M. ESCHALIER Romain : Cardiologie
M. MERLIN Etienne : Pédiatrie
Mme TOURNADRE Anne : Rhumatologie
M. DURANDO Xavier : Cancérologie
M. DUTHEIL Frédéric : Médecine et Santé au Travail
Mme FANTINI Maria Livia : Neurologie
M. SAKKA Laurent : Anatomie – Neurochirurgie
M. BOURDEL Nicolas : Gynécologie-Obstétrique
M. GUIEZE Romain : Hématologie
M. POINCLOUX Laurent : Gastroentérologie
M. SOUTEYRAND Géraud : Cardiologie

PROFESSEURS DES UNIVERSITES

M. CLEMENT Gilles : Médecine Générale
Mme MALPUECH-BRUGERE Corinne : Nutrition Humaine
M. VORILHON Philippe : Médecine Générale

PROFESSEURS ASSOCIES DES UNIVERSITES

Mme BOTTET-MAULOUBIER Anne : Médecine Générale
M. CAMBON Benoît : Médecine Générale

MAITRES DE CONFERENCES DES UNIVERSITES - PRATICIENS HOSPITALIERS

MAITRES DE CONFERENCES HORS CLASSE
Mme CHAMBON Martine : Bactériologie Virologie
Mme BOUTELOUP Corinne : Nutrition

MAITRES DE CONFERENCES DE 1ère CLASSE
M. MORVAN Daniel : Biophysique et Traitement de l'Image
Mle GOUMY Carole : Cytologie et Histologie, Cytogénétique
Mme FOGLI Anne : Biochimie Biologie Moléculaire
Mle GOUAS Laetitia : Cytologie et Histologie, Cytogénétique
M. MARCEAU Geoffroy : Biochimie Biologie Moléculaire
Mme MINET-QUINARD Régine : Biochimie Biologie Moléculaire
M. ROBIN Frédéric : Bactériologie
Mle VERONESE Lauren : Cytologie et Histologie, Cytogénétique
M. DELMAS Julien : Bactériologie
Mle MIRAND Andrey : Bactériologie Virologie
M. OUCHCHANE Lemlih : Biostatistiques, Informatique Médicale et Technologies de Communication
M. LIBERT Frédéric : Pharmacologie Médicale
Mle COSTE Karen : Pédiatrie
M. EVRARD Bertrand : Immunologie
Mle AUMERAN Claire : Hygiène Hospitalière
M. POIRIER Philippe : Parasitologie et Mycologie
Mme CASSAGNES Lucie : Radiologie et Imagerie Médicale
M. LEBRETON Aurélien : Hématologie

MAITRES DE CONFERENCES DE 2ème CLASSE
Mme PONS Hanaë : Biologie et Médecine du Développement et de la Reproduction
M. JABAUDON-GANDET Matthieu : Anesthésiologie – Réanimation Chirurgicale
M. BOUVIER Damien : Biochimie et Biologie Moléculaire
M. BUISSON Anthony : Gastroentérologie
M. COLL Guillaume : Neurochirurgie
Mme SARRET Catherine : Pédiatrie
M. MAQDASY Salwan : Endocrinologie, Diabète et Maladies Métaboliques
Mme NOURRISSON Céline : Parasitologie – Mycologie

MAITRES DE CONFERENCES DES UNIVERSITES

Mme BONHOMME Brigitte : Biophysique et Traitement de l'Image
Mme VAURS-BARRIERE Catherine : Biochimie Biologie Moléculaire
M. BAILLY Jean-Luc : Bactériologie Virologie
Mle AUBEL Corinne : Oncologie Moléculaire
M. BLANCHON Loïc : Biochimie Biologie Moléculaire
Mle GUILLET Christelle : Nutrition Humaine
M. BIDET Yannick : Oncogénétique
M. MARCHAND Fabien : Pharmacologie Médicale
M. DALMASSO Guillaume : Bactériologie
M. SOLER Cédric : Biochimie Biologie Moléculaire
M. GIRAUDET Fabrice : Biophysique et Traitement de l'Image
Mme VAILLANT-ROUSSEL : Hélène Médecine Générale
Mme LAPORTE Catherine : Médecine Générale
M. LOLIGNIER Stéphane : Neurosciences – Neuropharmacologie

Mme MARTEIL Gaëlle : Biologie de la Reproduction
M. PINEL Alexandre : Nutrition Humaine

MAITRES DE CONFERENCES ASSOCIES DES UNIVERSITES

M. TANGUY Gilles : Médecine Générale
M. BERNARD Pierre : Médecine Générale
Mme ESCHALIER Bénédicte : Médecine Générale
Mme RICHARD Amélie : Médecine Générale

DEDICACES

A Oleg, qui partage ma vie et me soutient au quotidien. Merci d'être là dans cette grande aventure de la vie.

A ma famille, particulièrement à mes parents, qui ont toujours cru en moi, et à mon frère, qui sait ce que signifie se battre pour vivre…

Aux amis de longue date, Nono, Emilie, Lilix, Caro, les jumelles et Bebe, souvent loin des yeux mais jamais loin du cœur !

Aux copines de médecine et pharmacie : Anne-Cho, Marie, Claire, Laure, Odile et Julianne. Que de bons souvenirs partagés ensembles, et encore beaucoup à vivre.

Aux médecins nucléaires de Jean Perrin, pour l'extraordinaire ambiance qu'ils font régner dans ce service, et particulièrement à ceux qui furent d'agréables cointernes. Si je devais remercier chacun d'entre vous, deux pages n'y suffiraient pas. J'espère que nous travaillerons longtemps ensemble.

Aux manipulateurs radio, radiopharmaciens et physiciens de Jean-Perrin, parce que si le service fonctionne, c'est grâce au travail d'équipe.

Aux professeurs Zanca et Mariano-Goulart, qui m'ont fait découvrir ma spécialité bien avant le début d'internat.

A Arnaud, pour avoir pris le temps de réaliser les nombreuses statistiques de cette thèse.

Aux copains de l'internat du Puy en Velay et d'Aurillac, pour les innombrables moments de joie que nous avons partagés.

Aux radiologues d'Issoire, pour leur accueil chaleureux et le superbe été que nous avons passé ensemble.

Au service de radiologie d'Aurillac, qui m'a permis de me perfectionner dans ce domaine, et surtout à Friemin, pour sa bonne humeur.

Aux médecins du service d'oncologie du Puy en Velay, qui m'ont permis d'acquérir de bonnes bases dans la prise en charge clinique des patients.

Aux infirmières d'oncologie du Puy en Velay, bien plus qu'une simple équipe de travail.

A l'équipe du Haras de Prat, qui me permet de vivre l'un de mes grands rêves d'enfant, et à celle du Batut, pour m'avoir tant appris à ce sujet.

REMERCIEMENTS

A Notre Président de Thèse :

A Madame le professeur PENAULT-LLORCA Frédérique,

Vous m'avez fait l'honneur d'accepter de présider le jury de ma thèse,

Je tiens à vous témoigner l'expression de mon profond respect,

Merci pour votre disponibilité et votre bienveillance.

A Notre Jury de Thèse :

A mon Directeur de Thèse, Monsieur le professeur CACHIN Florent,

Tu m'as fait l'honneur de me confier ce projet d'ampleur,

Tes conseils avisés m'ont permis de m'orienter dans ce sujet de recherche sans m'y perdre,

Merci pour ton implication dans cette thèse, pour ton engagement quotidien en tant qu'enseignant, ainsi que pour ton soutien concernant mes projets professionnels.

A Monsieur le professeur DURANDO Xavier,

Vous avez accepté de faire partie de ce jury, permettant ainsi d'apporter votre point de vue clinique sur ce projet,

Soyez-en remercié.

Au Docteur ORLHAC Fanny,

Je vous témoigne toute ma reconnaissance pour nos nombreux échanges de mails et discussion concernant l'analyse de texture,

Vos connaissances m'ont grandement aidée dans la réalisation de ce travail,

Je vous en remercie chaleureusement.

Table des matières

Dédicaces 7

Remerciements 8

Table des matières 9

Liste des tableaux et figures 10

Liste des abréviations 11

1. Introduction 13

2. Method 15

2.1. Population 15

2.2. Treatment 16

2.3. Clinical and Pathological Assessment 17

2.4. ^{18}FDG PET/CT Imaging 17

2.5. Statistical Analyses 22

3. Results 23

3.1. Population 23

3.2. Value of ^{18}FDG PET/CT for locoregional staging: Analysis by conventional and textural methods 24

3.3. Prediction of pathological response by ^{18}FDG PET/CT: Analysis by conventional and textural methods 26

4. Discussion 32

5. Conclusion 38

References 40

Annexe 1: Breast Cancer TNM classification (American Cancer Society)(3) 42

Annexe 2: Numbers and average values of baseline PET conventional and textural analysis: whole population 43

Annexe 3: Numbers and average values of interim PET conventional and textural analysis: whole population 45

Annexe 4: Principal Component Analysis (PCA) of conventionnal study 47

Annexe 5: Principal Component Analysis (PCA) of textural analysis 49

Annexe 6: Numbers and average values of baseline PET conventional and textural analysis, depending on pathological results 52

Annexe 7: Numbers and average values of interim PET conventional and textural analysis, depending on pathological results 55

Serment d'Hippocrate – Version longue 61

Serment d'Hippocrate – Version courte 62

Liste des tableaux et figures

Tableaux

Table I : Population characteristics 24
Table II: Results of conventional and texture analysis of PET0, depending on pathological complete response 27
Table III: Results of conventional metabolic evaluation on PET1, depending on pathological complete response 29
Table IV : Results of textural metabolic evaluation on PET1, depending on pathological complete response 30
Table V: Conventional analyses of PET0 in whole population 43
Table VI: First order textural analysis on PET0 in whole population 43
Table VII : Second order textural analysis on PET0 in whole population 43
Table VIII: Conventional analyses of PET1 in whole population 45
Table IX: First order textural analysis on PET1 in whole population 45
Table X: Second order textural analysis on PET1in whole population 46
Table XI: Differences in lymph nodal uptakes between PET0 and PET1 46
Table XII: Results of conventional and texture analysis of PET0: Grade 1 of Chevallier versus other patients 52
Table XIII : Results of conventional and texture analysis of PET0: Grade 1 versus Grade 2 versus Grade 3 of Chevallier 53
Table XIV: Results of PET0 nodal analysis 54
Table XV: Results of conventional analysis of PET1: Grade 1 of Chevallier versus other patients 55
Table XVI: Results of first order textural analysis of PET1: Grade 1 of Chevallier versus other patients 56
Table XVII: Results of second order textural analysis of PET1: Grade 1 of Chevallier versus other patients 56
Table XVIII: Results of conventional analysis of PET1: Grade 1 versus Grade 2 versus Grade 3 of Chevallier 57
Table XIX: Results of first order textural analysis of PET1: Grade 1 versus Grade 2 versus Grade 3 of Chevallier 58
Table XX: Results of second order analysis of PET1: Grade 1 versus Grade 2 versus Grade 3 of Chevallier 58
Table XXI: Results of PET1 nodal analysis - qualitative description 59
Table XXII: Results of PET1 nodal analysis - quantitative description 60

Figures

Figure 1 : Screen captures with LIFEx® software of one breast tumor, in PET0 and PET1 21
Figure 2 : Flow chart of studied population 23
Figure 3 : Example of Axial Fusion PET/CT views, Axial PET views and MIP views (right column) of one of our studied patients' exams 31

Liste des abréviations

5-FU: 5-Fluorouracil
CEA: Commissariat à l'Energie Atomique
CMR: Complete Metabolic Response
CR: Complete Response
DICOM: Digital Imaging and Communications in Medicine
EANM: European Association of Nuclear Medicine
^{18}FDG: ^{18}F-fluorodéoxyglucose
FEC 100: 5-Fluorouracil (5-FU): 500 mg/m^2, Epirubicin: 100 mg/m^2 and Cyclophosphamide: 500 mg/m^2
g: grams
HR: Hormonal Receptors
HER2: Human epidermal growth factor Receptor 2
HER+: overexpressing HER2 tumours
HGZE: High Grey-level Zone Emphasis
IHC: Immunohistochemistry
INCa: Institut National du Cancer
IV: intravenous/intravenously
LIFEx®: Local Image Features Extraction®
LGZE: Low Grey-level Zone Emphasis
LRE: Long Run Emphasis
MBq/Kg : Megabecquerels per kilograms
MIP: Maximum Intensity Projection
mL: milliliters
MRI: Magnetic Resonance Imaging
MV: Metabolic Volume
NeoTOP: Neoadjuvant phase II trial combining [3 FEC 100 followed by 3 docetaxel associated with trastuzumab plus pertuzumab] or [6 docetaxel, carboplatin associated with trastuzumab plus pertuzumab] according to TOP2A status in patients with operable, HER2-positive breast cancer
OR: Oestrogen Receptor
PCA: Principal Component Analysis
pCR: pathological Complete Response
PD: Progression Disease
PMD: Progression Metabolic Disease
PMR: Partial Metabolic Response
PR: Partial Response
PR: Progesterone Receptor
q3w: each three weeks
ROI: region of interest
SD: Stable Disease
SFMN: Société Française de Médecine Nucléaire
SMD: Stable Metabolic Disease
SUL: Lean body mass corrected SUV
SUL max: Maximum value of SUL in a ROI
SUL mean: Average value of SUL in a ROI

SUL peak: Average value of SUL in a 1 cm^3 sphere centred on the voxel corresponding to SUL max in a ROI
SUV: Standard Uptake Value
SUV max: Maximum value of SUV in a ROI
SUV mean: Average value of SUV in a ROI
SUV peak: Average value of SUV in a 1 cm^3 sphere centred on the voxel corresponding to SUV max in a ROI
SRE: Short Run Emphasis
PET/CT: Positon Emission Tomography/Computed Tomodensitometry
TLG: Total Lesion Glycolysis
TN: Triple Negative
TOP2A: Topoisomerase 2-alpha
WHO: World Health Organization

1. Introduction

Breast cancers have the highest incidence and mortality rates among women's solid malignant diseases. In France, between 1990 and 2018, its incidence is still increasing (more than 58000 new cases during that period), despite a high but decreasing mortality rate (12 004 death), probably due to a better organized screening during last decades(1).

Nowadays, its treatment is based on a multidisciplinary management, which can include surgery, medical oncology and radiation therapy, depending on breast cancer staging(2). This initial staging include TNM classification, updated in 2017 by the American Cancer Society(3) (reported in Annexe 1). Moreover, pathological tumours markers as Oestrogen Receptor (OR), Progesterone Receptor (PR), Human epidermal growth factor Receptor 2 (HER2) and proliferation rate (Ki67) are used to staging tumour aggressiveness, and can leading to a personalized management of breast cancer treatment, including endocrine therapy and/or HER2-directed Therapy(2).

Within the different kind of imaging modalities used in the management of breast cancer treatment, ^{18}F-fluorodeoxyglucose Positon Emission Tomography/Computed Tomodensitometry (^{18}FDG PET/CT) takes a more and more important place. Indeed, numerous studies had demonstrated the superiority of this exam's performance, regarding extra-axillar nodal staging, and detection of bone and visceral metastasis (excepted for brain)(4). Moreover, the prognostic value of initial staging by ^{18}FDG PET(4) and its performance in diagnosis of breast cancer relapse(4) had been highly validated.

French recommendations of the Institut National du Cancer (INCa) define it as an option in first intention initial staging for cT3-T4 and cN+ breast cancer, or after surgery, in case of macrometastatic lymph node disease(5). In 2018, it is recommended by the Société Française de Médecine Nucléaire (SFMN) for the initial staging of breast tumours clinically superior to

IIB stage, preferably before surgery, and can be proposed for the initial staging of breast tumours with a IIA clinical stage (T1N1 or T2N0), also preferably before surgery(6). It is recommended in case of suspected breast cancer relapse and in the restaging of proven breast cancer relapse(6). It can be proposed for the evaluation of systemic treatments in metastatic disease (particularly concerning bone metastasis)(6), and for the early evaluation of therapeutic response to neoadjuvant treatment, particularly for Triple Negative(TN) and HER2 overexpressing (HER2+) tumours(6). By the way, its predictive value of pathological response concerning this last indication remains uncertain. As well, even whether textural analysis of ^{18}FDG PET/CT has been evaluated for predicting the histological tumour type of breast cancer in some studies(7), only few analysed its ability to predict the pathological response to neoadjuvant therapy.

The main objective of this work was to determine the value of ^{18}FDG PET/CT for evaluation of disease staging and for prediction of early therapeutic response in neoadjuvant chemotherapy setting. Analysis were performed both by visual and conventional quantitative methods.

The secondary objective of this study was to analyse tumoral ^{18}FDG PET/CT textural features at baseline and in early evaluation response to neoadjuvant therapy

2. Method

2.1. Population

Studied population was extracted from the multicentric phase II trial NeoTOP (Neoadjuvant phase II trial combining [3 FEC 100 followed by 3 docetaxel associated with Trastuzumab plus Pertuzumab] or [6 Docetaxel, Carboplatin associated with Trastuzumab plus Pertuzumab] according to TOP2A status in patients with operable, HER2-positive breast cancer), promoted by Unicancer, whose rational was built by Clermont-Ferrand team, and whose final intent was to include 90 patients. Patients included was women over 18, and had a histologically confirmed breast cancer, with a clinical tumour superior to 1 cm (cT1c, cT2-3 or cT4a), any N status, and no clinically or radiologically detectable metastases (M0). Hormonal tumour receptors for T1c status were negative (both Oestrogen Receptor (OR) and Progesterone Receptor (PR) < 10% by Immunohistochemistry (IHC)), otherwise negative or positive. All tumours were HER2+ (i.e. IHC score 3+ or FISH/SISH/CISH positive). Performance status was ≤ 1 (according to World Health Organization (WHO) criteria). Hematologic, hepatic, renal and ionic patients' biology were normal at inclusion date. Cardiac ejection fraction, measured by MUGA or echography, was necessary superior to 50% within four weeks before inclusion. All patients agreed to use effective contraception during and for more than seven months after completion of study treatment. Finally, patients had to be able to comply with the protocol, must have signed a written informed consent form prior to any study specific procedures and must be affiliated to a Social Health Insurance.

Patients with bilateral or multifocal breast cancer, non-measurable tumour, inflammatory and/or overlooked forms (T4b or T4d) cancer, HER2- (i.e. IHC score 0 or 1+, or IHC score 2+ and FISH/SISH/CISH negative) or RH positive (OR or PR ≥ 10% by IHC) for T1c status were not included. Whether patients had a history of second cancer, including breast cancer, they were

not included, with exception of in situ cervical cancer or basocellular skin cancer which was regarded as cured. Pregnant women, women who was likely to become pregnant or was breast-feeding were not included. Patients with uncontrolled heart disease and for whom anthracyclines was contraindicated were not included.

Our population was included from January 12th of 2015 to December 3rd of 2018, and we collected data of the first scheduled interim analysis of NeoTOP trial.

2.2. Treatment

Patients were treated by six cycles of neoadjuvant chemotherapy, before undergoing mammary surgery. The therapeutic scheme was depending on the genetic Topoisomerase 2-alpha (TOP2A) amplification state.

Whether TOP2A was amplified, patients were treated with three cycles of FEC 100 (5-Fluorouracil (5-FU): 500 mg/m^2, Epirubicin: 100 mg/m^2 and Cyclophosphamide: 500 mg/m^2), administered intravenously (IV) each three weeks (q3w), followed by three cycles of Trastuzumab-Pertuzumab-Docetaxel (Trastuzumab 8 mg/kg loading dose administered intravenously (IV), followed by 6 mg/kg IV q3w in subsequent cycles ; Pertuzumab 840 mg loading dose administered IV followed by 420 mg IV q3w in subsequent cycles ; Docetaxel 75 mg/m^2 IV escalading at 100 mg/m^2 IV as tolerated, q3w).

Whether TOP2A was not amplified, patients were treated with TCHP, administered IV q3w for six cycles (Trastuzumab 8 mg/kg loading dose administered IV followed by 6 mg/kg IV q3w in subsequent cycles; Pertuzumab 840 mg loading dose administered IV followed by 420 mg IV q3w in subsequent cycles; Docetaxel 75 mg/m2 IV q3w; Carboplatin AUC 6 IV q3w).

Mammary surgery was performed within 28 days after completion of neoadjuvant treatment. If isotopic sentinel lymph node detection was performed during surgery, we noted it.

2.3. Clinical and Pathological Assessment

At baseline, clinical evaluations of tumoral and nodal involvement were fulfilled during four weeks before first cure of neoadjuvant therapy. Pathological results of biopsy were gathered, including tumour type and OR, PR and HER2 status.

Pathological response was scored on surgical sample according to Chevallier classification(8), whose pathological Complete Response (pCR) was corresponding to grades 1 (no residual tumour cell) and 2 (residual in situ carcinoma). Non-responders group corresponded to grades 3 (invasive carcinoma with stromal alterations, such as sclerosis or fibrosis) and 4 (no or few alterations in tumour appearance) of Chevallier classification. Whether an axillary lymph node dissection was performed during the surgery, the number of resected lymph nodes, tumour involved lymph nodes and carcinoma nodules were recorded.

2.4. ^{18}FDG PET/CT Imaging

Imaging acquisition

Two ^{18}FDG PET/CT exams were performed during neoadjuvant chemotherapy, one within seven days before starting treatment (baseline PET: PET0), the second 21 +/-3 days after the first cycle of chemotherapy (interim PET: PET1). Patients were instructed to fast and not consume beverages, except water, for at least four to six hours before administration of ^{18}FDG. Oral hydration was encouraged. Blood glucose level was measured before ^{18}FDG administration. Patient was rescheduled whether the glycaemia was greater than 11 mmol/L. Two to five MBq/Kg of ^{18}FDG was administrated, IV, for each ^{18}FDG PET/CT exam.

For PET0, a “whole body” standard acquisition was performed 60 min after injection. A dedicated mammary acquisition was followed exactly 90 minutes after tracer injection: two

beds of 5 min each with patient in prone position were acquired, centred on the mammary area.

For PET1, only a dedicated mammary acquisition was realized as same method described for PET 0.

Cross calibrations of all PET/CT devices and ^{18}FDG PET/CT acquisitions was performed according to guidelines of the European Association of Nuclear Medicine (EANM).

Whole body staging analysis

Whole body acquisition was analysed on Advantage Window Server 3.2 software (GE Healtcare®), to determine the metastatic staging. Uptake foci were considered as abnormal when their intensities were superior to liver uptake for lesions size superior to 1 cm or superior to vascular background for lesions inferior to 1 cm. Their localisations were recorded and a visual analysis was realized, staging these lesions in four categories:

- 0: no uptake
- 1: low uptake, inferior to liver background
- 2: moderate uptake, higher to liver background
- 3: high uptake

This visual staging was completed by a quantitative analysis, with measurement of SUV max, for suspected metastatic lesions.

Regional analysis of breast acquisition by conventional method: staging and metabolic response assessment

Conventional analysis of mammary acquisitions was also performed on Advantage Window Server 3.2 software.

Breast tumours localisations were collected and lesions were pooled in four categories, according to their visual uptake, in the same way as described for metastatic lesions.

Regional lymph nodes regions (ipsilateral axillary, intramammary and internal mammary chains) was visually analysed, and patients were sorted in two groups, according to absence or presence of lymph nodes uptakes suspicious of nodal disease.

For each breast and lymphonode uptake suspicious of tumour disease, we measured several parameters. Maximum Standard Uptake Value (SUV max)(9) was determined after automatic segmentation centred on the voxel with the highest intensity. SUV peak was the average uptake determined in a circular region of interest (1.2 cm in diameter) drawn automatically around SUV max voxel.

Moreover, three different tumoral ^{18}FDG mean uptakes were calculated: two based on growing region methods over 40% and 30% of the maximal intensity, respectively called SUV mean40% and SUV mean30%, and one by manual segmentation, named SUV meanMan.

For each SUV parameters, equivalent standardized patient lean mass (instead of weight), corresponding to SUL values(9), were also calculated.

The lesion with highest SUL peak on PET0 was considered as the main target for the evaluation, according to PERCIST criteria(10) .

All quantitative parameters were expressed in g/mL.

Finally, assessment of early metabolic response to chemotherapy was evaluated by comparison of PET0 and PET1 imaging in three ways:

- visual reading, scored as Progression Disease (PD), Stable Disease (SD), Partial Response (PR) and Complete Response (CR),

- quantitative analysis according to PERCIST criteria (variation of SUL Peak), scored as Progression Metabolic Disease (PMD), Stable Metabolic Disease (SMD), Partial Metabolic Response (PMR) and Complete Metabolic Response (CMR),

- variation of SUV and SUL values, according to pCR or not-pCR groups.

Textural Analysis of breast tumours

Textural analysis of mammary acquisitions was performed with Local Image Features Extraction (LIFEx)® software(11), whose associated intellectual property rights is held by the Commissariat à l'Energie Atomique (CEA).

On PET0 breast tumoral uptakes, a first ROI was drawn, by automatic segmentation defined at 40% of SUV max, named T40%. In an exploratory aim, we also analysed the peritumoral area, in a 5 mm thick region surrounding T40%, automatically drawn, named T40%Ring. With the purpose of performing a comparison between centres, we drew a spherical ROI of 10 cm^3 in the contralateral breast, named Contralat.

The same technic was applied to create ROI of residual tumours on PET1. Moreover, ROI corresponding to PET0 was manually placed on PET1 exam, when it was possible, for analysing textural parameters' variation in initial studied anatomic zones. These ROI were named T40%Repro and T40%ReproRing. Examples of each tumoral ROI drawn for textural analysis are illustrated with Figure 1. All ROI was resampled with voxels of 2 x 2 x 2 mm, and an absolute discretization of intensity in 128 grey levels, with a SUV max discretization fixed between 0 and 40 g/mL, was performed. Textural analysis wasn't performed if ROI volume was lower than 64 voxels, of if more than one Cluster was detected inside. Measurements of 15 first order (conventional) and 31 second order (textural) parameters were available on LIFEx®. In a synthetic purpose, we focused our analysis on 5 conventional indices and 6 textural indices,

known for their robustness(12)(13). Conventional indices measured were SUV max, SUV mean, SUV peak, Metabolic Volume (MV) and Total Lesion Glycolysis (TLG), which is defined with the following formula:

$$\mathrm{TGL} = \mathrm{MV} * \mathrm{SUV\ mean}$$

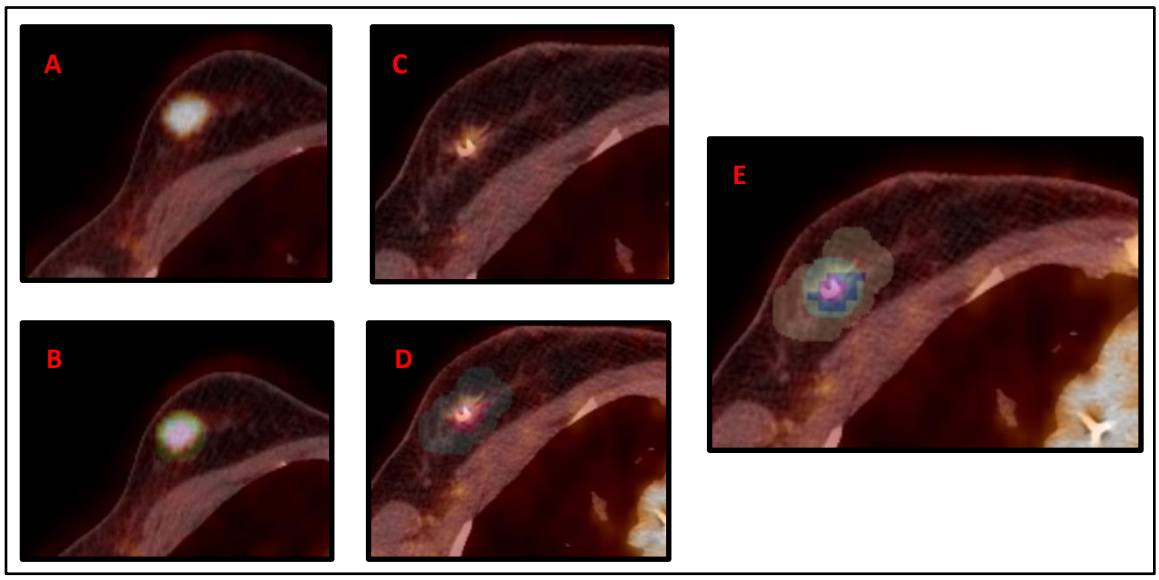

Figure 1 : Screen captures with LIFEx® software of one breast tumour, in PET0 and PET1.
A: Fusion PET/CT view of breast tumour on PET0.
B: Fusion PET/CT view of breast tumour on PET0, with coloured automatic ROI: T40% (pink) and T40%Ring (green).
C: Fusion PET/CT view of breast tumour on PET1.
D: Fusion PET/CT view of breast tumour on PET1, with coloured automatic ROI: T40% (pink) and T40%Ring (blue).
E: Fusion PET/CT view of breast tumour on PET1, with coloured automatic ROI an manually placed PET0 ROI: T40% (blue), T40%Ring (yellow), T40%Repro (pink) et T40% RingRepro (green). Due to a low uptake on PET1, automatic segmented volumes are wider than PET0 ones.

Textural indices measured were Homogeneity, Entropy, Short Run Emphasis (SRE), Long Run Emphasis (LRE), Low Grey-level Zone Emphasis (LGZE) and High Grey-level Zone Emphasis (HGZE). Inside a ROI, Homogeneity represents the uniformity of voxels' intensity repartition, whereas Entropy corresponds to its randomness. SRE and LRE give information about fields of homogeneous intensity, respectively in a short area or in a long area. LGZE and HGZE bring information about respectively low grey-level and high grey level voxels' intensity repartition. Variations of conventional and textural parameters between PET0 and PET1 were expressed in percentage.

2.5. Statistical Analyses

Statistical analyses were performed with R® software. Exact Fisher Test was used to detect dependence between pCR and qualitative variables: Visual response and PERCIST response. For conventional measures, Wilcoxon Mann Whitney Test was used to detect dependence between pCR and quantitative variables, concerning their initial values and variations between PET0 and PET1.

Regarding Textural Analysis, a t Student Test was performed if variables had a normal distribution. When variances were not equal between groups, a t Welsh Test was used. If observed data had not a normal distribution, a non-parametric Wilcoxon Mann Whitney Test (U test) was performed.

We performed a Principal Component Analysis (PCA) to detect a centre effect concerning quantitative variables of tumoral lesions measured in conventional analysis, and to study the correlation between them (details in Annexe 4). We also performed a PCA on the textural analysis of contralateral breast, to detect a centre effect in that kind of ROI, which was supposed to be more reproducible between patients (details in Annexe 5).

3. Results

3.1. Population

86 patients were included in NeoTOP trial at the time of our study. 43 PET0 exams were conventionally studied, among which 40 exams were analysable for textural parameters. Results and mean values of quantitative parameters of this first screening are reported in Annexes 2 and 3. 43 patients were not analysable for PET0 for this work, because of not transferred data, acquisitions issues or incomplete DICOM (Digital Imaging and Communications in Medicine) parameters. Pathological results were available for 27 studied patients, whose formed our effective population, and 23 of them were analysable for textural parameters. Among them, 22 were evaluable conventionally on PET1, and 16 were evaluable by texture analysis on PET1. Absence of revaluation on PET1 was also induced by technical acquisition issues, lack of data transfer, or incomplete DICOM parameters. Figure 2 summarizes the flow chart of our study.

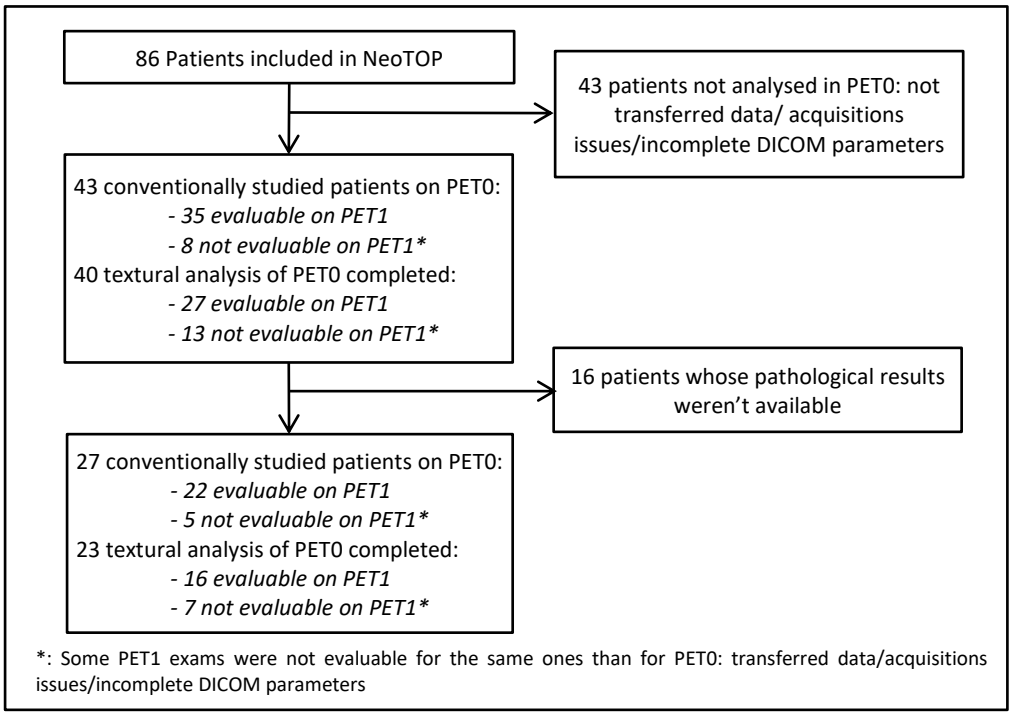

Figure 2 : Flow chart of studied population

Our effective population was 53 years old (39-74), with a similar proportion of menopaused and not menopaused women. PET exams were acquired in eight centres. The histological type was ductal most of tumours: 24 patients (88,9%). None patient was presenting a lobular tumour. 15 patients (55,6%) had tumours with negative hormonal receptors. None of patients presented focal uptakes suspected of metastatic disease on PET 0 whole body acquisition. Chevallier classification was known for 25 patients in our database.

Characteristics of our population are summarized on Table I.

Anthropometric values	**Moy (N=27)**	**Min-Max**
Age (years)	53	39-74
Weight (kg)	62,7	40-91
Height (cm)	160,6	146-172
Menopausal state	**N**	**%**
Menopaused	14	51,9
Not menopaused	13	48,1
Total	**27**	**100**
PET Center	**N**	**%**
Clermont-Ferrand	8	29,6
Montpellier	6	22,2
Angers	3	11,1
Limoges	3	11,1
Saint-Herblain	3	11,1
Strasbourg	4	14,8
Total	**27**	**100**
Histological tumoral type	**N**	**%**
Ductal	24	88,9
Micropapillary breast cancer	1	03,7
Invasive Carcinoma	2	07,4
Total	**27**	**100**
Tumoral Hormonal Receptors	**N**	**%**
OR - and PR -	15	55,6
OR + and PR +	11	40,7
OR + and PR -	1	03,7
Total	**27**	**100**

Table I : Population characteristics

3.2. Value of ^{18}FDG PET/CT for locoregional staging: Analysis by conventional and textural methods

On PET0, 21 patients (81%) presented a tumour with high uptake; visual grade 3, and 4 patients' tumours (16%) had a moderate uptake, visual grade 2. None of patients presented tumours with low or absent uptake. Three patients had two suspicious focal uptakes in the

same breast. The average of tumoral SUV max of our population was 12,87+/-7,85 g/mL. The PCA performed on breast tumoral lesions did not evidence a centre effect concerning conventional quantitative tumoral parameters, and all of them was highly correlated (minimum 0,89). Synthetic schemes of that PCA are reported in Annexe 4.

Concerning first order measured parameters, average of tumours' TLG, automatically segmented at 40% of SUV max, was 37,04+/-45,16, average of SUV max of peritumoral zones (T40%Ring) was 7,57+/-4,93 g/mL, and average TLG of peritumoral zones was 30,07+/-23,17 mL. SUV Peak was not measurable for T40%Ring ROI. Concerning second order parameters of tumoral lesions, we found higher values of Entropy, LRE and HGZE than Homogeneity, SRE and LGZE ones on PET0. Moreover, PCA performed on Contralateral breast showed a correlation between SUV max, SUV peak, SUV mean, TLG, Entropy, SRE and HGZE. Most of these parameters had a reverse correlation with LRE and Homogeneity, and some of them with LGZE. By the way, the PCA also showed a significant centre effect existing in our textural measurement ($p = 0.0286$).

Among the 27 patients of our final population, 15 showed regional lymphnode uptakes suspected of malignancy on PET0, which quantitative characteristics are reported in Annexe 6, due to their low number.

20 patients (74,1%) were clinically staged N0, and among them, 11 had suspicious regional nodal uptakes on PET0. Six of the seven patients classed as clinical N1 showed suspicious regional nodal uptakes. In total, a discordance between PET and clinical regional nodal staging was present for 10 patients (37%).

Axillary lymph node clearance was not performed for 15 patients. Isotopic sentinel lymph node detection during surgery was realized for 13 of them. Among this group, five patients had suspicious nodal uptakes on PET0, whose one staged cN1 and four staged cN0 at baseline,

and eight patients was staged N0 on PET0, whose one staged cN1 and seven staged cN0 at baseline. Two patients did not underdo axillary clearance or isotopic sentinel lymph node detection, and these two did not showed suspicious lymph nodes uptakes on PET0 and was staged cN0 at baseline.

Twelve patients underwent an axillary lymph node clearance, and among them, only two had a pathological nodal involvement on surgical sample. Both had suspicious lymph nodes uptakes on PET0, one of them staged cN1 and the second one cN0 at baseline. Eight clearance did not demonstrate pathological nodal involvement. Two of them was staged N0 with PET0 and clinical baseline staging, and six had suspicious nodal uptakes in PET0: two staged cN0 and four staged cN1 at baseline. Pathological nodal involvement was unknown for two patient cases who had an axillary lymph node clearance. Numbers, average values, and known pathological state of PET0 lymph nodes analysis are reported in Annexe 6.

3.3. Prediction of pathological response by ^{18}FDG PET/CT: Analysis by conventional and textural methods

Predictive value of initial PET

18 patients (72%) were considered in pCR according to Chevallier classification (Grades 1+2) and seven patients (28%) were considered as no responders (Grade 3). None of patients was classified as Grade 4 of Chevallier. Two of patients presenting two suspicious foci uptakes in the same breast were Grade 1, and the third was Grade 3.

There was not significant statistical difference between responders and no responders, concerning initial values of conventional and textural PET0 parameters, as well for tumoral ROI than T40%Ring ROI ($p>0,2$ for all of them).

Numbers, averages values and statistics corresponding to PET0 are reported in Table II. In order to avoid redundancies, SUV max, SUV mean and SUV peak measured with LIFEx® for T40% ROI are not reported.

	Total			pCR			No pCR			Statistics	
Visual Analysis	**N**		**%**	**N**		**%**	**N**		**%**	**-**	
0	0		0	0		0	0		0		
1	0		0	0		0	0		0		
2	4		16	3		12	1		4	-	
3	21		81	15		60	6		24		
Total	***25***		***100***	***18***		***72***	***7***		***28***		
SUV (g/mL)	**N**	**Moy**	**Σ**	**N**	**Moy**	**Σ**	**N**	**Moy**	**Σ**	**P**	**IC95%**
Max	25	12.87	7.85	18	12.34	7.58	7	14.23	8.99	0.701	(-7.54 – 4.5)
Peak	24	8.49	5.58	17	8.32	6.09	7	8.90	4.47	0.576	(-5.57 – 3.13)
Mean40%	24	8.00	4.79	17	7.85	4.96	7	8.35	4.71	0.757	(-4.47 – 3.35)
Mean30%	25	6.70	4.31	18	6.46	4.47	7	7.30	4.14	0.534	(-4.09 – 2.45)
MeanMan	25	3.91	2.13	18	3.94	2.34	7	3.84	1.59	0.883	(-1.69 – 1.67)
SUL(g/mL)	**N**	**Moy**	**Σ**	**N**	**Moy**	**Σ**	**N**	**Moy**	**Σ**	**p**	**IC95%**
Max	25	8.97	4.79	18	8.80	2.34	7	9.41	4.64	0.790	(-4.42 – 3.47)
Peak	24	5.90	3.51	17	5.88	4.97	7	5.97	2.53	0.664	(-3.11 – 2.67)
Mean40%	24	5.54	2.93	17	5.54	3.91	7	5.55	2.45	0.901	(-2.83 – 2.57)
Mean30%	25	4.71	2.72	18	4.66	3.18	7	4.85	2.17	0.762	(-2.64 – 2.24)
MeanMan	25	2.72	1.32	18	2.78	1.49	7	2.57	0.76	0.976	(-1.02 – 1.31)
Texture 1st order	**N**	**Moy**	**Σ**	**N**	**Moy**	**σ**	**N**	**Moy**	**Σ**	**p**	**IC95%**
T40%											
TLG	22	37.04	45.16	16	39.02	52.08	6	31.77	19.57	0.641	(-29 – 32.8)
MV (mL)	22	4.21	2.84	16	4.22	3.03	6	4.18	2.54	0.978	(-2.87 – 2.95)
T40% Ring											
SUV mean	23	2.27	1.20	17	2.15	1.00	6	2.61	1.71	0.806	(-1.61 – 1.02)
SUV max	23	7.57	4.93	17	7.07	4.67	6	8.99	5.82	0.392	(-6.84 – 3.41)
TLG	23	30.07	23.17	17	28.51	24.64	6	34.51	19.70	0.293	(-28.28 – 13)
MV (mL)	23	12.62	6.50	17	12.22	6.90	6	13.73	5.61	0.636	(-8.04 – 5.03)
Texture 2nd order	**N**	**Moy**	**Σ**	**N**	**Moy**	**σ**	**N**	**Moy**	**Σ**	**p**	**IC95%**
T40%											
Homogeneity	17	0.31	0.12	11	0.33	0.14	6	0.29	0.09	0.733	(-0.1 – 0.16)
Entropy	17	2.32	0.42	11	2.31	0.49	6	2.33	0.27	0.928	(-0.48 – 0.45)
SRE	17	0.95	0.04	11	0.94	0.05	6	0.96	0.02	0.481	(-0.06 – 0.03)
LRE	17	1.30	0.34	11	1.35	0.41	6	1.20	0.13	0.513	(-0.16 – 0.36)
LGZE	17	0.01	0.01	11	0.01	0.02	6	0.00	0.00	0.884	(0 – 0.01)
HGZE	17	1042.42	1199.12	11	1110.99	1324.69	6	916.69	1030.72	0.961	(-640 – 1409.84)
T40% Ring											
Homogeneity	23	0.46	0.14	17	0.47	0.15	6	0.42	0.13	0.464	(-0.09 – 0.19)
Entropy	23	1.97	0.51	17	1.92	0.53	6	2.12	0.46	0.422	(-0.71 – 0.31)
SRE	23	0.89	0.07	17	0.89	0.07	6	0.91	0.04	0.806	(-0.08 – 0.05)
LRE	23	1.85	0.67	17	1.91	0.75	6	1.69	0.40	0.944	(-0.46 – 0.88)
LGZE	23	0.04	0.04	17	0.05	0.05	6	0.02	0.02	0.421	(0 – 0.05)
HGZE	23	177.43	157.36	17	160.46	139.94	6	225.51	206.25	0.392	(-192.4 – 90.5)

Table II: Results of conventional and texture analysis of PET0, depending on pathological complete response

There was not significant difference between Grade 1 of Chevallier group and others patients concerning conventional and textural quantitative parameters analysis on PET0. Same results were obtained with comparison of our three groups: Grade 1 vs Grade 2 vs Grade 3. Results of these complementary analyses are reported in Annexe 6.

Predictive value of interim PET

Metabolic evaluation on PET1 was performed for 21 patients.

In PET visual analysis, three patients (14,3%) was in CR, 17 (81,0%) was in PR and one of them (4,8%) showed a SD. None was visually progressing in PET1 evaluation. There was not significant difference between pathological responders and no responders concerning our visual analysis (p=1). Both patient with two suspicious breast uptakes on PET0 was in partial metabolic response on PET1 and Grade 1 of Chevallier, and the third wasn't evaluable on PET1.

All quantitative conventional parameters measured on tumoral ROI decreased between PET0 and PET1, with an average of -55+/-18% concerning SUV max. Whatever studying parameters, tumoral ^{18}FDG decrease was similar in Chevallier defined response group (p>0,5 for all of them).

PERCIST evaluation could be performed on 20 patients and classified one (5%) in complete metabolic response, eight (40%) in partial metabolic response, 10 in stable metabolic disease (50%) and one (5%) in progression disease. One patient could not be evaluated with PERCIST method, due to parameters issues in PET1 data (SUL peak not calculable). There was not significant difference between pathological responders and no responders concerning PERCIST evaluation (p=1). Numbers, averages values and statistics corresponding to conventional PET evaluation are reported in Table III.

Textural evaluation on PET1 exams could be performed on 13 patients' exams. Most of first order parameters decreased between PET0 and PET1, excepting some metabolic volumes, which increased: 07,06+/-107,83% for T40%, 39,25+/-122,73% for T40%Ring, 14,76+/-28,02% for T40%Repro. TLG of lesions decreased of 65,89+/-20,25% with automatic segmentation and 67,01+/-14,08% with manual placement of initial ROI. TLG of peritumoral zone decreased of

24,84+/-64,39% with automatic segmentation and 53,36+/-11,27% with manual replacement of initial ROI.

	Total			pCR			No pCR			Statistics	
Visual analysis	**N**		**%**	**N**		**%**	**N**		**%**	**p**	
CR	3		14,3	3		14,3	0		0,0		
PR	17		81,0	13		62,9	4		19,0		
SD	1		4,8	1		4,8	0		0,0	**1**	
PD	0		0	0		0	0		0,0		
Total	***21***		***100***	***17***		***81,0***	***4***		***19,0***		
ΔSUV	**N**	**Moy (%)**	**σ**	**N**	**Moy (%)**	**Σ**	**N**	**Moy (%)**	**σ**	**p**	**IC95%**
Max	19	-55	18	15	-54	18	4	-60	16	0.578	(-0.27 – 0.16)
Peak	18	-54	16	14	-53	17	4	-57	14	0.639	(-0.24 – 0.16)
Mean40%	16	-57	16	12	-56	16	4	-60	18	0.678	(-0.24 – 0.17)
Mean30%	13	-55	15	10	-55	17	3	-53	07	0.843	(-0.21 – 0.26)
MeanMan	21	-49	21	17	-49	24	4	-48	07	0.977	(-0.25 – 0.26)
ΔSUL	**N**	**Moy (%)**	**σ**	**N**	**Moy (%)**	**Σ**	**N**	**Moy (%)**	**σ**	**p**	**IC95%**
Max	19	-55	18	15	-54	18	4	-60	16	0.544	(-0.27 – 0.15)
Peak	18	-54	16	14	-53	17	4	-58	14	0.574	(-0.25 – 0.15)
Mean40%	16	-57	16	12	-55	17	4	-60	18	0.613	(-0.25 – 0.16)
Mean30%	13	-55	17	10	-56	19	3	-54	09	0.897	(-0.23 – 0.26)
MeanMan	20	-43	18	16	-41	20	4	-49	07	0.437	(-0.29 – 0.13)
PERCIST	**N**		**%**	**N**		**%**	**N**		**%**	**p**	
CMR	1		5	1		5	0		0		
PMR	8		40	4		20	4		20		
SMD	10		50	10		50	0		0	**1**	
PD	1		5	1		5	0		0		
Total	***20***		***100***	***16***		***80***	***4***		***20***		

Table III: Results of conventional metabolic evaluation on PET1, depending on pathological complete response

Concerning second order textural parameters, we showed an increase of Homogeneity, LRE and LGZE, meanwhile Entropy, SRE and HGZE decreased, as well for tumoral than peritumoral region, and both for automatic segmentation and manually replacement methods, assessing a decrease of tumoral heterogeneity as well as uptake, due to first cure of chemotherapy.

By the way, none textural parameters' variation was significantly different between pCR and no pCR groups (p>0,2 for all of them). Numbers, averages values and statistics corresponding to textural evaluation are reported in Table IV. As well as for PET0 results, SUV max, SUV mean and SUV peak measured with LIFEx® for T40% ROI aren't reported.

There was not significant difference between Grade 1 of Chevallier group and others patients concerning visual, PERCIST, conventional quantitative or textural metabolic evaluations on

PET1. It was the same for the comparison of conventionnal parameters of our three groups: Grade 1 vs Grade 2 vs Grade 3. Results of these complementary analysis are reported in Annexe 7.

	Total			pCR			No pCR			Statistics	
ΔTexture 1st ordre	**N**	**Moy (%)**	**σ**	**N**	**Moy (%)**	**σ**	**N**	**Moy (%)**	**σ**	**p**	**IC95%**
T40%											
TLG	12	-65.89	20.25	8	-66.20	24.98	4	-65.27	6.78	0.924	(-22.41 – 20.56)
Volume	12	07.06	107.83	8	03.00	133.53	4	-27.17	14.89	0.799	(-53.59 – 338.43)
T40% Ring											
SUV Mean	15	-44.84	18.22	10	-42.84	22.09	5	-48.85	5.83	0.437	(-10.36 – 22.39)
SUV Max	15	-54.89	17.33	10	-53.97	20.93	5	-56.75	7.70	0.513	(-14.38 – 10.34)
TLG	15	-24.84	64.39	10	-25.57	59.28	5	-23.37	81.25	0.768	(-77.9 – 64.31)
Volume	15	39.25	122.73	10	31.24	99.18	5	55.28	173.49	0.953	(-216.58 – 161.7)
T40% Repro											
SUV Mean	10	-70.42	13.45	5	-72.63	17.14	5	-68.21	10.05	0.632	(-24.91 – 16.08)
SUV Max	10	-58.83	20.28	5	-56.65	27.54	5	-61.01	12.47	0.841	(-20.12 – 49.59)
SUVPeak 0,5mL	6	-61.00	25.28	4	-63.86	31.94	2	-55.28	5.96	0.740	(-75.48 – 58.32)
SUVPeak 1mL	5	-56.50	20.56	3	-56.28	28.85	2	-56.85	4.97	0.981	(-68.37 – 69.52)
TLG	10	-67.01	14.08	5	-70.67	16.82	5	-63.34	11.38	0.443	(-28.27 – 13.62)
Volume	10	14.76	28.02	5	12.87	36.00	5	16.64	21.50	0.846	(-47.01 – 39.47)
T40% Ring Repro											
SUV Mean	11	-52.12	11.29	6	-53.14	15.30	5	-50.89	4.76	0.745	(-18.31 – 13.82)
SUV Max	11	-40.16	27.17	6	-37.82	34.31	5	-42.98	18.85	0.772	(-33.87 – 44.19)
TLG	11	-53.36	11.27	6	-53.79	15.47	5	-52.86	4.25	0.893	(-17.14 – 15.28)
Volume	11	-02.27	06.91	6	-0.94	8.81	5	-3.86	4.09	0.515	(-6.81 – 12.65)
ΔTexture 2nd ordre	**N**	**Moy (%)**	**σ**	**N**	**Moy (%)**	**σ**	**N**	**Moy (%)**	**σ**	**p**	**IC95%**
T40%											
Homogeneity	10	48.16	31.70	6	54.87	40.35	4	38.10	8.76	0.365	(-25.5 – 59.04)
Entropy log10	10	-24.80	14.81	6	-27.06	18.01	4	-21.39	9.59	0.762	(-33.84 – 13.99)
SRE	10	-08.13	13.39	6	-10.49	17.29	4	-4.59	3.39	0.914	(-38.3 – 5.6)
LRE	10	71.99	158.90	6	101.82	205.99	4	27.25	24.13	0.990	(-42.64 – 478.19)
LGZE	10	485.75	319.40	6	485.97	331.88	4	485.42	349.97	0.998	(-503.71 – 504.82)
HGZE	10	-74.24	10.07	6	-72.98	24.81	4	-76.12	7.55	0.610	(-18.38 – 45.28)
T40% Ring											
Homogeneity	15	45.15	21.91	10	45.34	26.58	5	44.76	9.46	0.964	(-26.32 – 27.48)
Entropy log10	15	-33.73	14.80	10	-34.04	16.64	5	-33.12	11.99	0.915	(-19.09 – 17.25)
SRE	15	-15.83	14.77	10	-15.56	15.72	5	-16.37	14.37	0.859	(-14.01 – 19.16)
LRE	15	111.29	144.62	10	109.31	161.26	5	115.24	121.08	0.679	(-190.43 – 81.01)
LGZE	15	482.78	395.15	10	397.79	288.95	5	652.77	551.79	0.253	(-715.52 – 205.57)
HGZE	15	-68.28	20.25	10	-66.26	24.18	5	-72.34	9.38	0.859	(-12.94 – 26.17)
T40% Repro											
Homogeneity	10	77.70	62.88	5	95.89	77.85	5	59.52	44.80	0.392	(-56.26 – 129.01)
Entropy log10	10	-24.79	17.85	5	-30.64	22.28	5	-18.93	11.63	0.328	(-37.62 – 14.2)
SRE	10	-11.52	13.40	5	-16.07	18.33	5	-6.97	4.08	0.841	(-37.78 – 8.17)
LRE	10	87.30	127.34	5	132.67	174.68	5	41.93	28.72	0.548	(-49.1 – 381.33)
LGZE	10	2508.36	2141.76	5	2937.59	2798.79	5	2079.14	1423.83	0.990	(-1975.22 – 6169.25)
HGZE	10	-82.70	11.75	5	-82.89	15.53	5	-82.51	8.32	0.963	(-18.54 – 17.79)
T40% Ring Repro											
Homogeneity	11	61.33	28.37	6	65.43	36.54	5	56.41	16.96	0.626	(-31.37 – 49.41)
Entropy log10	11	-33.34	12.55	6	-34.08	15.59	5	-32.45	9.37	0.844	(-19.69 – 16.45)
SRE	11	-20.96	12.10	6	-22.39	15.11	5	-19.24	8.60	0.69	(-20.46 – 14.16)
LRE	11	136.75	81.06	6	151.10	101.99	5	119.53	52.40	0.549	(-83.02 – 146.17)
LGZE	11	516.55	476.84	6	557.66	516.68	5	467.21	478.73	0.772	(-594.68 – 775.57)
HGZE	11	-60.55	27.15	6	-57.58	35.41	5	-64.11	15.71	0.713	(-32.36 – 45.42)

Table IV : Results of textural metabolic evaluation on PET1, depending on pathological complete response

In a synthesis purpose, and due to their low numbers, lymphnode regional metabolic evaluations are not detailed here (reported in Annexe 7). By the way, we can note that the

only patient classed in stable metabolic disease concerning her nodal involvement on PET1, and which presented an unusual high uptake on PET0 (SUV max = 39,76 g/mL), had a pathological nodal involvement diagnosed on her axillary clearance.

In Figure 3, we show the example of a patient classed in PR concerning her tumour, but in CR concerning her nodal uptake.

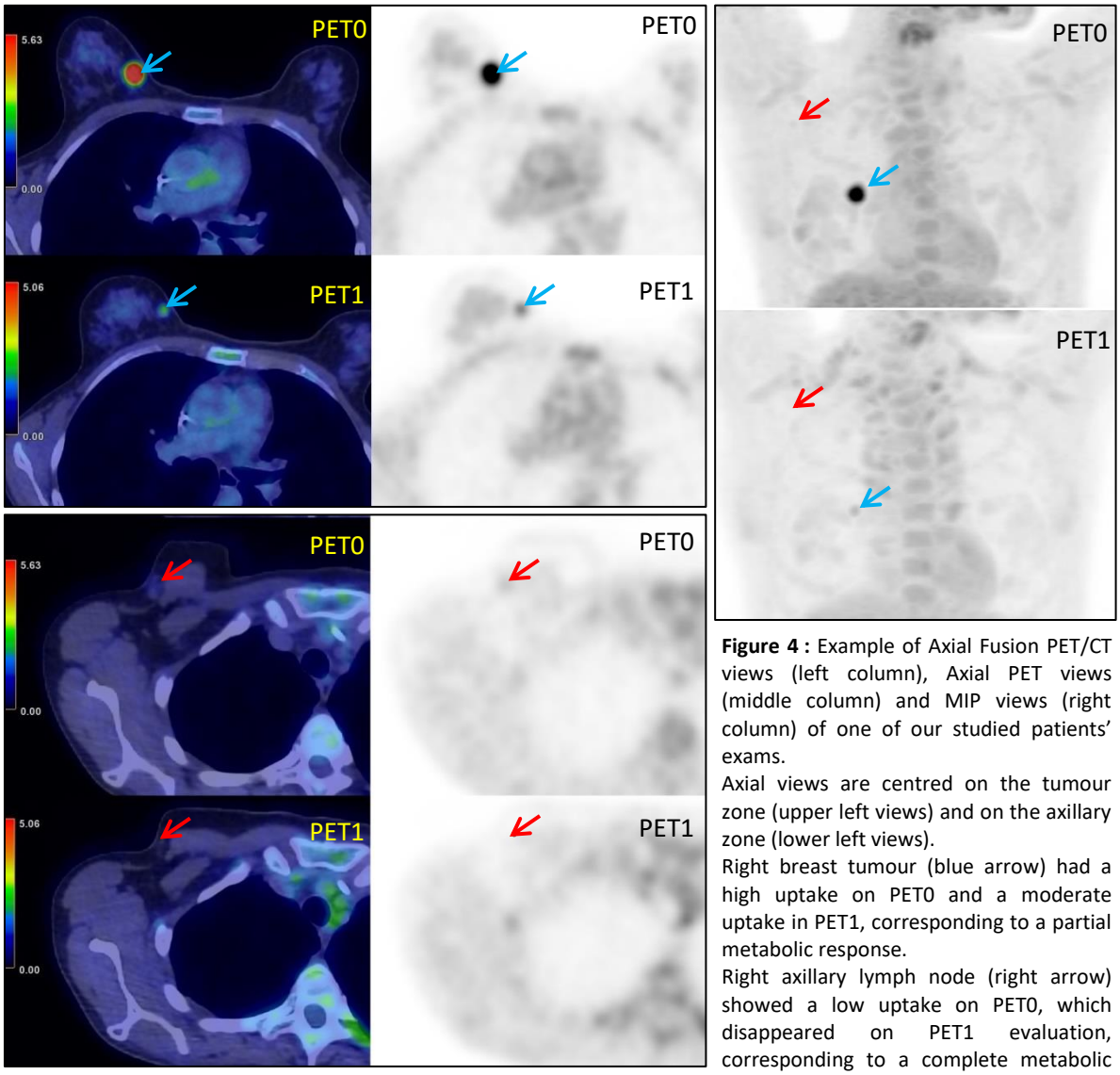

Figure 4 : Example of Axial Fusion PET/CT views (left column), Axial PET views (middle column) and MIP views (right column) of one of our studied patients' exams.
Axial views are centred on the tumour zone (upper left views) and on the axillary zone (lower left views).
Right breast tumour (blue arrow) had a high uptake on PET0 and a moderate uptake in PET1, corresponding to a partial metabolic response.
Right axillary lymph node (right arrow) showed a low uptake on PET0, which disappeared on PET1 evaluation, corresponding to a complete metabolic response.

4. Discussion

Conventional PET assessment and pathological complete response

We did not evidence any significant differences between pathological responders and no responders concerning initial PET local assessment and interim PET therapeutic response by conventional evaluation. It could be explained by the low statistical power of our population, particularly concerning no responders: seven patients (28%). Double inhibition of HER2 receptor associated with chemotherapy in neoadjuvant treatment could explain our high pCR rate. Moreover, it is important to underline the absence of Grade 4 of Chevallier in our population, suggesting some partial pathologic response even for patients considered as no responders. Indeed, variations of conventional parameters between PET0 and PET1 seem to suggest a therapeutic effect of neoadjuvant chemotherapy for the whole studied population. At last, we performed PET/CT evaluation after only one treatment cycle, possibly too early for observing a difference between pCR and no pCR groups.

Interestingly, all conventional parameters were correlated, suggesting that measurement of only one suffices to inform about ^{18}FDG uptake. Indeed, the measurement of SUV max, which is usually practiced in Nuclear Medicine, seems to be an easy and fast way to gather this information.

Our results are in contradiction with Avathaxer trial, which studied the relationship between ^{18}FDG PET/CT and pathological response(14). In this study, an adjunction of Bevacizumab to the initial therapy (Docetaxel) + Trastuzumab) was performed in one subgroup of non-responding patients in PET evaluation, leading to a better pCR rate that the subgroup of non-responding metabolic patients, who was treated with Docetaxel and Trastuzumab: 43,8% versus 24% respectively. Moreover, these two subgroups had a lower pCR rate than the PET-responding one (53,6%).

Textural PET features and pathological complete response

Our tumoral ROI on PET0 showed high values of Entropy and HGZE, associated with low values of Homogeneity and LGZE, which seems to be coherent with tumoral microenvironment characteristics, known for being composed of different kind of cells with high metabolism(15). Surprisingly, in our study, the values of LRE was higher that SRE ones in PET0, suggesting the presence of a majority large areas with homogeneous intensity fields in tumoral sites, compared with short areas. By the way, textural parameters measured in our study after one cure of neoadjuvant treatment varied as expected (13), with a decrease of Entropy, SRE,HGZE and respectively an increase of Homogeneity, LRE and LGZE indexes. Correlations or reverse correlations between textural parameters existing in Contralateral breast ROI supported the logic of these variations induced by neoadjuvant treatment**.** However, we did not evidence any significant differences between pathological responders and no responders concerning textural evaluation, on baseline as well as interim PET.

To our best knowledge, this study is the first to measure ^{18}FDG accumulation and variation in peritumoral zones before and after one cure of chemotherapy, as well as its potential ability to predict pCR. On PET0, average SUV max was 7,57+/-4,93 g/mL, and average TLG was 30,07 +/-23,17, which decreased on PET1, as well for automatic than manually placed ROI. We measured high values of Entropy, LRE and HGZE and low values of Homogeneity, SRE and LGZE on PET0. Increase of Homogeneity, LRE and LGZE, and decrease of Entropy, SRE and HGZE were measured on PET1, as well as for automatic than manually placed ROI. Unfortunately, no relationship between these parameters and pCR was demonstrated in our study. This point should be studied further, particularly with a comparison to pathological results. Imaging of tumoral and peritumoral microenvironment remains of interest, especially in view of development of specific therapies targeting microenvironment(15).

The centre effect existing in textural analysis underline the difficulties inherent to use this technic in multicentric studies. Low reproducibility is due to differences of PET/CT devices' resolution and reconstruction technics. Moreover, textural analysis' comparison between studies is affected by the use of different kind of segmentation method, variations in textural indexes definition and small size of the majority of studies (12,13,16,17). Furthermore, some results of our textural study question about the validity of our measurement, particularly concerning variations of PET0 ROI volumes placed manually on PET1 (14,76+/-28,02% for T40%Repro), which logically should not vary. Indeed, our results have to be carefully interpreted.

Even if relationship between ^{18}FDG PET/CT and pCR following neoadjuvant therapies in breast cancer have already been investigated, results of different studies are discordant and suffer from reproducibility issues. In their study, Soussan et al. found a moderate correlation between Homogeneity, Entropy and Metabolic Volume PET parameters, and the association of HGRE with SUV max was higher than SUV max alone to predict the aggressiveness of histological type(7). By the way, the method was not the same as ours, a Nestle segmentation being used.

Few studies evaluated the predictive value of PET/CT textures parameters to predict pCR in HER+ breast cancers. As for our study, Cheng et al. did not observe a link between absolute values of conventional and textural parameters of initial PET and pCR. On a cohort of 31 HER2+ breast cancers patients, they only demonstrate a moderately predictive value of pCR relative to the variations of one texture parameter (Skewness) and SUV max, between 2 PET exams(18). Moreover, they also measured a high rate of pCR in their HER2+ group (71%). By the way, PET evaluation was performed after two cures of chemotherapy (Paclitaxel+Carboplatine+Trastuzumab), and the segmentation method was also different.

Yoon et al. found in univariate analysis a link between 15 textural parameters and pathological response to neoadjuvant therapy, including Entropy, Homogeneity, LRE and High-intensity large-zone emphasis (like HGZE)(19). Unfortunately, in multivariate analysis, only one parameter (Number nonuniformity) was significantly associated with pathological response. The study did not mention the differences between subgroup of breast cancer, and response to chemotherapy was lower for HER+ patients than in our study (21 responders versus 11 non responders). Lymphnode involvement at baseline was also higher in nonresponders group (91,9% versus 73,9%), what could significate a more aggressive tumour behaviour, and consequently a higher risk of relapse. Moreover, segmentation method was different from ours (threshold with SUV superior to 2,5). In their study, Lee et al. showed a link between numerous texture parameters and pCR in their global population, including Entropy, SRE and LRE, however not in HER2+ population, composed by 70 patient (35 responders and 35 non-responders)(20). Furthermore, segmentation technic was not fully explained in this article. Lemarignier et al.'s therapeutic scheme had some similarity with our study(21): the neoadjuvant treatment associated Epirubicine, Cyclophosphamide, Docetaxel and Trastuzumab. But pCR rate was 12%. They showed that TGL and SUV max was associated with pathological complete response but none of textural parameters, as Homogeneity and Entropy, measured in manually drawn ROI, achieve significant correlation with pCR. This cohort included OR positive breast cancer, and none analysis was performed in HER+ subgroup.

Lee et al. determine three models of textural patterns with machine learning methods and showed that clinicopathological data associated with texture parameters was better that clinicopathological data alone for the prediction of pCR(20). However, machine learning methods are tools not currently used in clinical practice.

Comparison with clinical and radiological findings

In our study, we found a quite high level of discordance between Clinical and Metabolic staging for lymphnode disease (37%). It should have been suitable to compare it with conventional radiological finding. ^{18}FDG PET/CT showed best performance in nodal staging, according to the metaanalysis of Groheux et al.(4). Radiological evaluation modalities could also be compared with textural analysis technics. Yoon et al. found no link between MRI texture and pCR, in a multivariate analysis(19). Unfortunately, at time of our study, radiological data relative to lymphnode disease were unknown. Moreover, tumoral radiological evaluation and biological data were available for only few patients.

It is also important to underline that some suspicious PET lesions could have modified the management of some patients of our study, particularly for patients harbouring multifocal ^{18}FDG breast abnormalities, which modify surgery protocol.

Prognostic value of 18FDG PET/CT?

Finally, value of ^{18}FDG PET as prognostic or predictive factor for predicting patient's survival will be next evaluated, when survival data will be available. Prognostic value of ^{18}FDG PET/CT, including textural parameters, has already been investigated. Yoon et al. found that a tumoral high-intensity zone emphasis measured on baseline PET of breast cancer treated with neoadjuvant chemotherapy and surgery was associated with a higher risk of recurrence (19). Ha et al. analysed numerous parameters, with a machine learning system, which classed patients in three Clusters(22). pCR rate in this study was 23%, and the recurrence rate was 5,5%, with 4 patients, who were not in pCR. The Cluster 1 was associated with a better survival than Clusters 2 and 3.

Thus, follow up our population, with the aim of analysing the prognostic value of ^{18}FDG PET/CT, is of interest.

Limits

Our study suffers from insufficient statistical power, due to its low number of patients. It is an intermediary analysis, and results will be compared at the end of this trial.

Moreover, we underlined the difficulties inherent to multicentric trials concerning textural analysis.

Finally, the fact that analysis did not take into account TOPA2 status can bring a selection bias in our study, that we will analyse at the end of NeoTOP trial.

5. Conclusion

This work is an ancillary study of multicentric and prospective « NeoTOP » trial, promoted by Unicancer, whose rational was built by Clermont-Ferrand team. 90 Patients presenting a breast cancer with positive HER2 receptor and treated with a neoadjuvant therapy will be included. Among 27 patients, we did not find a link between pathological response and tumoral uptake of ^{18}F-fluorodeoxyglucose, before treatment or after one neoadjuvant course. Values of baseline PET's tumoral quantitative parameters was highly correlated, without any centre effect. Textural analysis of tumoral uptake before treatment and variation after one course was not correlated with pathological response. These results should be compared with final analysis encompassing the whole population. Finally, the prognostic value of tumoral uptake and lymphnode disease on ^{18}FDG PET/CT will be assessed when overall survival and survival without relapse data will be available.

Conclusion

Ce travail est une analyse intermédiaire de l'étude prospective multicentrique « NEOTOP » promue par Unicancer et dont le rationnel a été construit par l'équipe de Clermont-Ferrand. 90 patientes présentant un cancer du sein exprimant le récepteur HER2 et bénéficiant d'un traitement néoadjuvant seront à termes incluses. Chez 27 patientes, il n'a pas été mis en évidence de lien entre la réponse histologique et la fixation tumorale du 18F-fluorodeoxyglucose visualisée avant traitement ou après une cure. Les valeurs des paramètres quantitatifs de l'évaluation initiale étaient fortement corrélées entre elles, sans effet centre mis en évidence. L'analyse texturale de la fixation tumorale avant traitement et sa variation après une cure n'étaient pas corrélées avec la réponse anatomopathologique. Ces résultats seront à comparer à ceux de l'analyse finale, qui portera sur l'ensemble de la population. Enfin la valeur pronostique de la fixation tumorale et de l'atteinte ganglionnaire en TEP 18 FDG sera évaluée lorsque les données de survie sans récidive et de survie globale seront disponibles.

Le Doyen de l'UFR de Médecine,

Pierre CLAVELOU

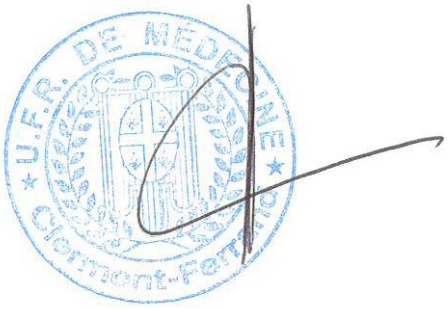

La Présidente du Jury,

Frédérique PENAULT-LORCA

References

1. Binder-foucard F, Belot A, Delafosse P, Remontet L, Woronoff A-S, Bossard N. Estimation nationale de l ' incidence et de la mortalité par cancer en France entre 1980 et 2012. Inst Veill Sanit. 2013;

2. McDonald ES, Clark AS, Tchou J, Zhang P, Freedman GM. Clinical Diagnosis and Management of Breast Cancer. J Nucl Med [Internet]. 2016;57(Supplement_1):9S-16S. Available from: http://jnm.snmjournals.org/cgi/doi/10.2967/jnumed.115.157834

3. American Cancer Society. Breast Cancer Stages [Internet]. 2017. Available from: https://www.cancer.org/cancer/breast-cancer/understanding-a-breast-cancer-diagnosis/stages-of-breast-cancer.html

4. Groheux D, Cochet A, Humbert O, Alberini J-L, Hindie E, Mankoff D. 18F-FDG PET/CT for Staging and Restaging of Breast Cancer. J Nucl Med [Internet]. 2016;57(Supplement_1):17S-26S. Available from: http://jnm.snmjournals.org/cgi/doi/10.2967/jnumed.115.157859

5. Et S, Des VIE. BREAST 2012 INCA questions actualite cancer du sein infiltrant non metastatique. 2012;

6. SFMN. RBP utilisation TEP en cancerologie. 2018; Available from: https://www.sfmn.org/drive/SFMN/GUIDES DE PROCEDURES/GuidesEtRecommandation_PublicWeb/RBP utilisation TEP en cancerologie synthese_V1.pdf

7. Soussan M, Orlhac F, Boubaya M, Zelek L, Ziol M, Eder V, et al. Relationship between tumor heterogeneity measured on FDG-PET/CT and pathological prognostic factors in invasive breast cancer. PLoS One. 2014;9(4):1–7.

8. Veyret C, Levy C, Chollet P, Merrouche Y, Roche H, Kerbrat P, et al. Inflammatory breast cancer outcome with epirubicin-based induction and maintenance chemotherapy: Ten-year results from the French Adjuvant Study Group GETIS 02 trial. Cancer. 2006;107(11):2535–44.

9. Buvat I. Outils de quantification pour l'imagerie TEP au FDG [Internet]. Available from: http://www.guillemet.org/irene/coursem/INSTN2011.pdf

10. Wahl RL, Jacene H, Kasamon Y, Lodge MA. From RECIST to PERCIST : Evolving Considerations for PET Response Criteria in Solid Tumors. J Nucl Med. 2009;50(Suppl 1):1–50.

11. Nioche C, Orlhac F, Boughdad S, Reuze S, Goya-Outi J, Robert C, et al. Lifex: A freeware for radiomic feature calculation in multimodality imaging to accelerate advances in the characterization of tumor heterogeneity. Cancer Res [Internet]. 2018;78(16):4786–9. Available from: www.lifexsoft.org

12. Orlhac F, Soussan M, Maisonobe J-A, Garcia CA, Vanderlinden B, Buvat I. Tumor Texture Analysis in 18F-FDG PET: Relationships Between Texture Parameters, Histogram

Indices, Standardized Uptake Values, Metabolic Volumes, and Total Lesion Glycolysis. J Nucl Med. 2014;55(3):414–22.

13. Orlhac F, Nioche C, Soussan M, Buvat I. Understanding changes in tumor texture indices in PET: A comparison between visual assessment and index values in simulated and patient data. J Nucl Med. 2017;58(3):387–92.

14. Coudert B, Pierga JY, Mouret-Reynier MA, Kerrou K, Ferrero JM, Petit T, et al. Use of [18F]-FDG PET to predict response to neoadjuvant trastuzumab and docetaxel in patients with HER2-positive breast cancer, and addition of bevacizumab to neoadjuvant trastuzumab and docetaxel in [18F]-FDG PET-predicted non-responders (AVATAXHER): An . Lancet Oncol. 2014;15(13):1493–502.

15. Klemm F, Joyce JA. Microenvironmental regulation of therapeutic response in cancer. Trends Cell Biol [Internet]. 2015;25(4):198–213. Available from: http://dx.doi.org/10.1016/j.tcb.2014.11.006

16. Hatt M, Tixier F, Pierce L, Kinahan PE, Le Rest CC, Visvikis D. Characterization of PET/CT images using texture analysis: the past, the present… any future? Eur J Nucl Med Mol Imaging. 2017;44(1):151–65.

17. Chalkidou A, O'Doherty MJ, Marsden PK. False discovery rates in PET and CT studies with texture features: A systematic review. PLoS One. 2015;10(5):1–18.

18. Cheng L, Zhang J, Wang Y, Xu X, Zhang Y, Zhang Y, et al. Textural features of 18 F-FDG PET after two cycles of neoadjuvant chemotherapy can predict pCR in patients with locally advanced breast cancer. Ann Nucl Med. 2017;31(7):544–52.

19. Yoon HJ, Kim Y, Chung J, Kim BS. Predicting neo-adjuvant chemotherapy response and progression-free survival of locally advanced breast cancer using textural features of intratumoral heterogeneity on F-18 FDG PET/CT and diffusion-weighted MR imaging. Breast J. 2019;25(3):373–80.

20. Lee H, Lee DE, Park S, Kim TS, Jung SY, Lee S, et al. Predicting response to neoadjuvant chemotherapy in patients with breast cancer: Combined statistical modeling using clinicopathological factors and FDG PET/CT texture parameters. Clin Nucl Med. 2019;44(1):21–9.

21. Lemarignier C, Martineau A, Teixeira L, Vercellino L, Espié M, Merlet P, et al. Correlation between tumour characteristics, SUV measurements, metabolic tumour volume, TLG and textural features assessed with 18F-FDG PET in a large cohort of oestrogen receptor-positive breast cancer patients. Eur J Nucl Med Mol Imaging. 2017;44(7):1145–54.

22. Ha S, Park S, Bang JI, Kim EK, Lee HY. Metabolic Radiomics for Pretreatment 18F-FDG PET/CT to Characterize Locally Advanced Breast Cancer: Histopathologic Characteristics, Response to Neoadjuvant Chemotherapy, and Prognosis. Sci Rep [Internet]. 2017;7(1):1–11. Available from: http://dx.doi.org/10.1038/s41598-017-01524-7

Annexe 1: Breast Cancer TNM classification (American Cancer Society)(3)

T	**TX**	Primary tumor cannot be assessed.	
	T0	No evidence of primary tumor.	
	Tis	Carcinoma in situ (DCIS, or Paget disease of the nipple with no associated tumor mass),	
	T1	(includes T1a, T1b, and T1c)**:** Tumor is 2 cm (3/4 of an inch) or less across.	
	T2	Tumor is more than 2 cm but not more than 5 cm (2 inches) across.	
	T3	Tumor is more than 5 cm across.	
	T4	(includes T4a, T4b, T4c, and T4d)**:** Tumor of any size growing into the chest wall or skin. This includes inflammatory breast cancer.	
N	**NX**	Nearby lymph nodes cannot be assessed (for example, if they were removed previously).	
	N0	Cancer has not spread to nearby lymph nodes.	**N0(i+):** The area of cancer spread contains less than 200 cells and is smaller than 0.2 mm. The abbreviation "i+" means that a small number of cancer cells (called isolated tumor cells) were seen in routine stains or when a special type of staining technique, called immunohistochemistry, was used.
			N0(mol+): Cancer cells cannot be seen in underarm lymph nodes (even using special stains), but traces of cancer cells were detected using a technique called *RT-PCR*. RT-PCR is a molecular test that can find very small numbers of cancer cells. (This test is not often used to find breast cancer cells in lymph nodes because the results do not influence treatment decisions.)
	N1	Cancer has spread to 1 to 3 axillary (underarm) lymph node(s), and/or tiny amounts of cancer are found in internal mammary lymph nodes (those near the breast bone) on sentinel lymph node biopsy.	**N1mi:** Micrometastases (tiny areas of cancer spread) in the lymph nodes under the arm. The areas of cancer spread in the lymph nodes are at least 0.2mm across, but not larger than 2mm.
			N1a: Cancer has spread to 1 to 3 lymph nodes under the arm with at least one area of cancer spread greater than 2 mm across.
			N1b: Cancer has spread to internal mammary lymph nodes on the same side as the cancer, but this spread could only be found on sentinel lymph node biopsy (it did not cause the lymph nodes to become enlarged).
			N1c: Both N1a and N1b apply.
	N2	Cancer has spread to 4 to 9 lymph nodes under the arm, or cancer has enlarged the internal mammary lymph nodes.	**N2a:** Cancer has spread to 4 to 9 lymph nodes under the arm, with at least one area of cancer spread larger than 2 mm.
			N2b: Cancer has spread to one or more internal mammary lymph nodes, causing them to become enlarged.
	N3	Any of the following :	**N3a:** Cancer has spread to 10 or more axillary lymph nodes, with at least one area of cancer spread greater than 2 mm, **or** Cancer has spread to the lymph nodes under the collarbone (infraclavicular nodes), with at least one area of cancer spread greater than 2 mm.
			N3b: Cancer is found in at least one axillary lymph node (with at least one area of cancer spread greater than 2 mm) and has enlarged the internal mammary lymph nodes, **or** Cancer has spread to 4 or more axillary lymph nodes (with at least one area of cancer spread greater than 2 mm), and tiny amounts of cancer are found in internal mammary lymph nodes on sentinel lymph node biopsy.
			N3c: Cancer has spread to the lymph nodes above the collarbone (supraclavicular nodes) with at least one area of cancer spread greater than 2 mm.
M	**MX**	Distant spread (metastasis) cannot be assessed.	
	M0	No distant spread is found on x-rays (or other imaging tests) or by physical exam.	**cM0(i+):** Small numbers of cancer cells are found in blood or bone marrow (found only by special tests), or tiny areas of cancer spread (no larger than 0.2 mm) are found in lymph nodes away from the underarm, collarbone, or internal mammary areas.
	M1	Cancer has spread to distant organs (most often to the bones, lungs, brain, or liver).	

Annexe 2: Numbers and average values of baseline PET conventional and textural analysis: whole population

48 breast focal uptakes were measured on 43 patients analysable on PET0.

39 Patients had a visual score of 3, six had a visual score of 2, and three had a visual score of 1. None patient was visually classed scored as 0.

Values of conventional parameters of breast uptakes are reported in the following table:

	SUV					SUL				
	Max	Peak	Mean 40%	Mean 30%	Mean Man	Max	Peak	Mean 40%	Mean 30%	Mean Man
Number	48	47	44	43	48	48	47	44	43	48
Average (g/mL)	10,50	7,02	6,80	6,09	3,30	7,22	4,76	4,62	4,13	2,26

Table V: Conventional analyses of PET0 in whole population

First and second order textural analysis of this population are reported in two following table.

		SUV Mean (g/mL)	SUV Max (g/ml)	SUVpeak sphere 0.5mL	SUVpeak sphere 1mL	TLG	Volume (mL)
T40%	Number	41	41	28	28	41	41
	Average	6,715	11,518	9,252	6,567	32,269	4,196
T40% Ring	Number	43	43	-	-	43	43
	Average	1,973	6,432	-	-	26,159	12,570

Table VI: First order textural analysis on PET0 in whole population

		GLCM Homogeneity (=Inverse difference)	Entropy log10	GLRLM SRE	GLRLM LRE	GLZLM LGZE	GLZLM HGZE
T40%	Number	32	32	32	32	32	32
	Average	0,351	2,187	0,929	1,449	0,016	740,552
T40% Ring	Number	43	43	43	43	43	43
	Average	0,493	1,834	0,871	2,286	0,065	139,459

Table VII : Second order textural analysis on PET0 in whole population

In whole population, 22 patients showed suspicious regional lymph node uptakes on PET0. Most of them were in level 1 and 2 of Berg classification(8), sometimes at the limit between intramammary and homolateral axillary areas. However, two patients showed suspicious uptakes in internal mammary lymphatic chains, and one patient had a suspicious uptake at the level 3 of Berg classification.

44 suspicious lymph nodes uptakes were measured at PET0, showing average values of 6,56 g/mL for SUV max, 3,43 g/mL for SUV peak, 4,42 g/mL for SUL max and 2,21 g/ml for SUL peak.

Annexe 3: Numbers and average values of interim PET conventional and textural analysis: whole population

37 mammary breast uptakes were measured on 35 patients analysable on PET1.

In interim PET, 13 patients were visually classed in score 3, 12 in score 2, five in score 1 and five in score 0.

Values of conventional parameters of breast uptakes are reported in the following table:

		SUV					SUL				
		Max	Peak	Mean 40%	Mean 30%	Mean Man	Max	Peak	Mean 40%	Mean 30%	Mean Man
Difference	Number	30	29	25	19	31	30	29	25	19	31
	Average(%)	-51,98	-52,85	-53,79	-50,33	-42,36	-52,29	-53,03	-53,87	-50,86	-42,40

Table VIII: Conventional analyses of PET1 in whole population

23 Patients were analysable for textural features in PET1. Results of these analysis are reported on two following tables.

			SUV mean	SUV max	SUV peak sphere 0.5mL	SUV peak sphere 1mL	TLG	Volume (mL)
Différence	**T40%**	Number	23	23	14	7	23	23
		Average(%)	-51,06	-50,06	-49,60	-53,01	-58,06	-4,85
	T40% Ring	Number	25	25	-	-	25	25
		Average(%)	-40,64	-50,68	-	-	-30,30	20,75
	T40% Repro	Number	15	15	9	7	15	8
		Average(%)	-69,03	-59,79	-61,63	-57,76	-64,17	27,72
	T40% Ring Repro	Number	16	16	-	-	16	8
		Average(%)	-50,17	-42,26	-	-	-48,31	4,14

Table IX: First order textural analysis on PET1 in whole population

			GLCM Homogeneity (=Inverse difference)	Entropy log10	GLRLM SRE	GLRLM LRE	GLZLM LGZE	GLZLM HGZE
Différence	T40%	Number	17	17	17	17	17	17
		Average(%)	41,00	-23,40	-9,17	63,39	406,72	-66,80
	T40% Ring	Number	25	24	25	25	25	25
		Average(%)	40,23	-32,89	-14,95	96,89	400,87	-62,12
	T40% Repro	Number	14	14	14	14	14	14
		Average(%)	74,51	-26,41	-15,15	106,90	2290,40	-81,97
	T40% Ring Repro	Number	16	16	16	16	16	16
		Average(%)	56,73	-36,80	-24,65	156,73	513,12	-61,08

Table X: Second order textural analysis on PET1in whole population

On PET1 evaluation, 11 patients showed suspicious lymph node uptakes. Variation of quantitative parameters corresponding to lymph node uptakes are reported on the following table.

		SUV		SUL	
		Max	Peak	Max	Peak
Difference	Number	12	11	12	11
	Average(%)	-51,58	-46,29	-52,09	-46,50

Table XI: Differences in lymph nodal uptakes between PET0 and PET1

Annexe 4: Principal Component Analysis (PCA) of conventionnal study

PCA is performed on all standard normal distributions.

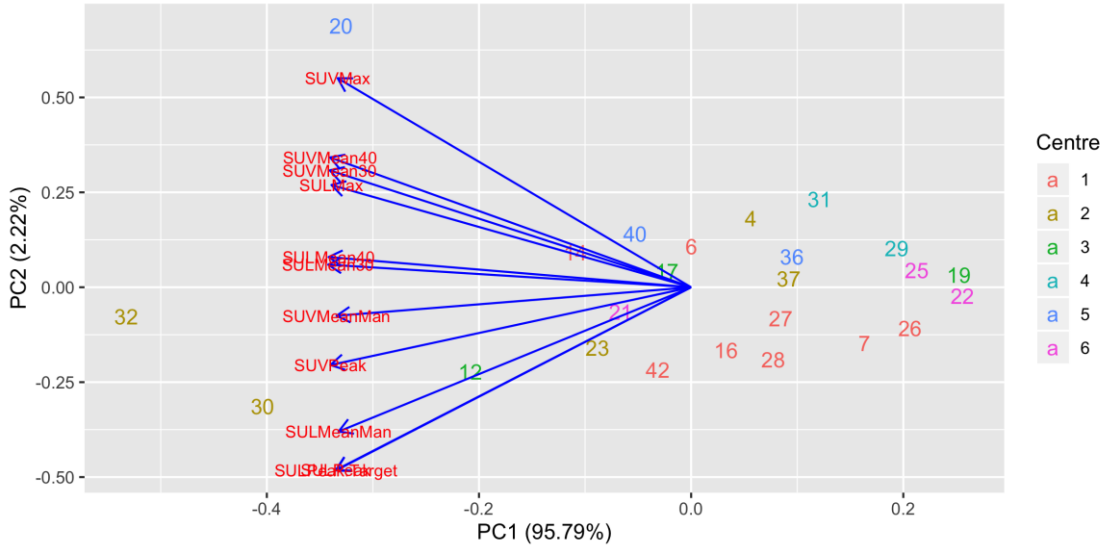

Axis 1 explain 95,79% of PET0 data variance. All parameters are well projected on this axis.

Variables are well correlated between them (correlation minimum = 0.89).

Correlation Matrix between variables:

	SUV Max	SUVP eak	SUVMea n40	SUVMea n30	SUVMean Man	SUL Max	SULP eak	SULMea n40	SULMea n30	SULMean Man	SULPeak.T arget
SUVMax	1.00	0.94	0.99	0.99	0.93	0.98	0.89	0.96	0.96	0.89	0.89
SUVPeak	0.94	1.00	0.97	0.97	0.96	0.95	0.98	0.96	0.97	0.95	0.98
SUVMean 40	0.99	0.97	1.00	1.00	0.96	0.98	0.92	0.98	0.98	0.92	0.92
SUVMean 30	0.99	0.97	1.00	1.00	0.96	0.98	0.93	0.98	0.98	0.93	0.93
SUVMean Man	0.93	0.96	0.96	0.96	1.00	0.92	0.92	0.94	0.94	0.98	0.92
SULMax	0.98	0.95	0.98	0.98	0.92	1.00	0.94	0.99	0.99	0.92	0.94
SULPeak	0.89	0.98	0.92	0.93	0.92	0.94	1.00	0.96	0.96	0.95	1.00
SULMean40	0.96	0.96	0.98	0.98	0.94	0.99	0.96	1.00	1.00	0.94	0.96
SULMean30	0.96	0.97	0.98	0.98	0.94	0.99	0.96	1.00	1.00	0.95	0.96
SULMean Man	0.89	0.95	0.92	0.93	0.98	0.92	0.95	0.94	0.95	1.00	0.95
SULPeak.T arget	0.89	0.98	0.92	0.93	0.92	0.94	1.00	0.96	0.96	0.95	1.00

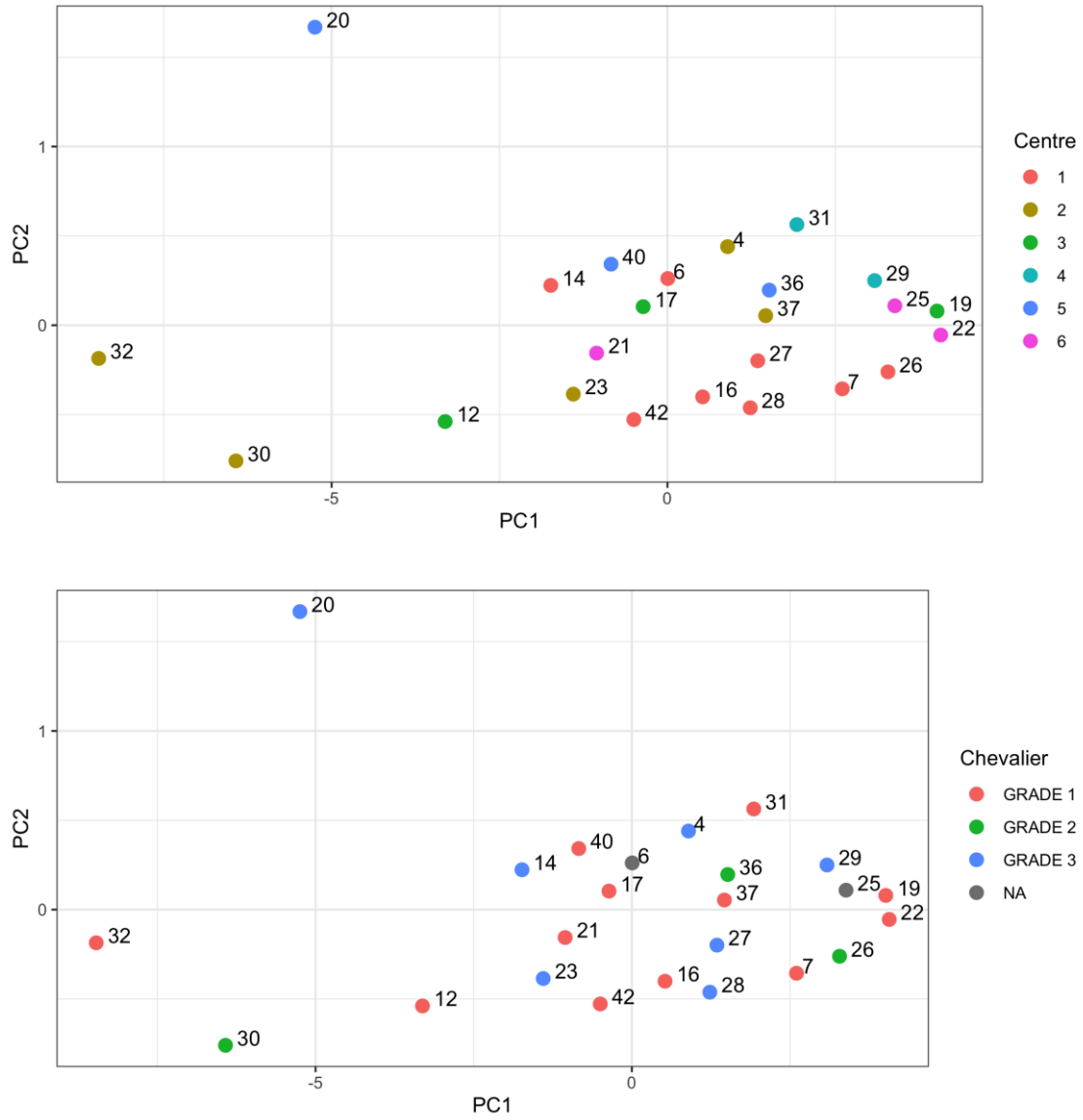

Patients 20,30 and 32 have unusual profile compared with the rest of population. They have the most intense uptakes.

Annexe 5: Principal Component Analysis (PCA) of textural analysis

PCA is performed on all standard normal distributions of Contralat ROI on PET0.

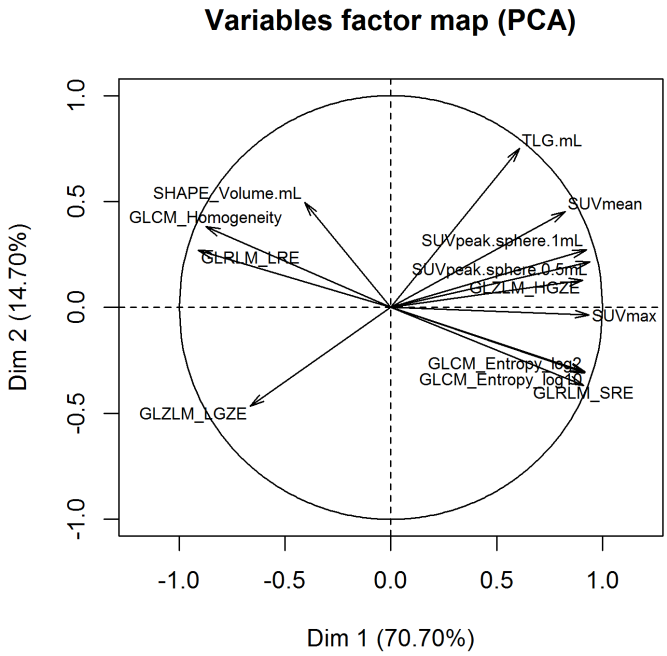

Axis 1 explain 70,7% of textural data variance and Axis 2 explain only 14,7% of data variance.

We reported correlation between variables and PCA components, to find which ones are the best to explain PCA axes.

	Dim.1	Dim.2
SUVmean	0.8237866	0.4525362
SUVmax	0.9363659	-0.0343620
SUVpeak.sphere.0.5mL	0.9404745	0.2149445
SUVpeak.sphere.1mL	0.9229273	0.2725652
TLG.mL	0.6079671	0.7510612
SHAPE_Volume.mL	-0.4073417	0.4952218
GLCM_Homogeneity	-0.8737047	0.3819765
GLCM_Entropy_log10	0.9167491	-0.3039514
GLCM_Entropy_log2	0.9156127	-0.3086459
GLRLM_SRE	0.9111683	-0.3679715
GLRLM_LRE	-0.9091142	0.2701077
GLZLM_LGZE	-0.6651451	-0.4660539
GLZLM_HGZE	0.9067632	0.1285998

SUV max and SUV peak (sphere.0.5mL) have the best projection on Axis 1, with a correlation of 0.936 between SUV max and Axis 1. Only TLG is well projected on Axis 2.

Some of parameters are highly correlated.

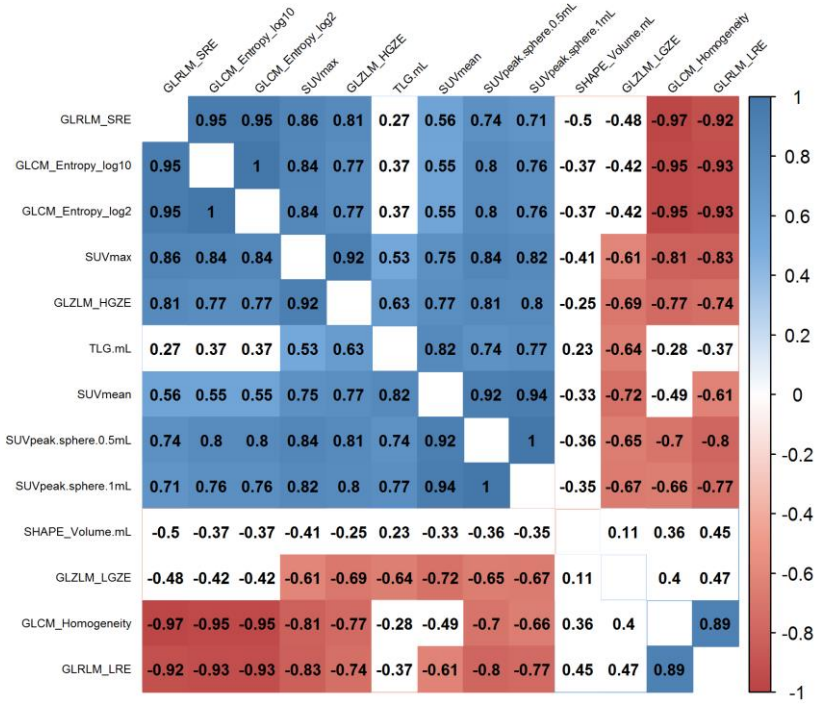

This graphic shows Pearson correlations between variables: in blue positive correlations and in red negative correlations. Only correlations significantly different from null correlation are coloured. SHAPE Volume is the only parameter no correlated with others variables.

Projection points, representing patients, are coloured differently according to their centre with the aim of representing a potential « centre effect ».

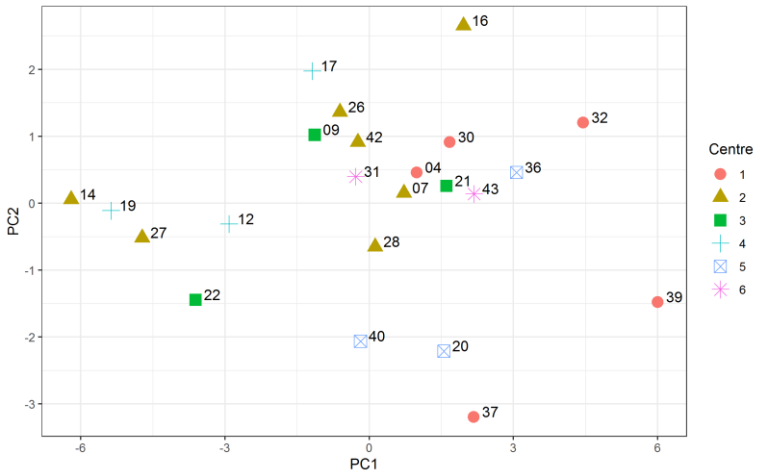

Data from different centres seems to be different, probably because of data variability.

Patients 32 and 39 have a high Contralat SUV Max. Patient 37 have a low TLG, opposite to patient 16.

This tendency is observable with a Manova performed on two first Axis of PCA. The difference between centres is significantly different on the first axis of PCA ($p=0.0286$). A “Centre effect” is observed.

Annexe 6: Numbers and average values of baseline PET conventional and textural analysis, depending on pathological results

We performed a complementary statistical analysis on our baseline PET population, between patients corresponding to Grade of 1 of Chevallier and the group composed by Grade 2 and Grade 3.

Exact test of Fisher was used for qualitative variables and Wilcoxon Mann Whitney test for quantitative ones. Results of these analyses are reported on following table.

	Grade 1			Grade 2+3			Total			Statistic	
Visual analysis	**N**		**%**	**N**		**%**	**N**		**%**		
0	0		0	0		0	0		0		
1	0		0	0		0	0		0		
2	1		4	3		12	4		16	-	
3	13		52	8		32	21		81		
Total	***14***		***56***	***11***		***44***	***25***		***100***		
SUV (g/mL)	**N**	**Moy**	**σ**	**N**	**Moy**	**σ**	**N**	**Moy**	**σ**	**p**	**IC95%**
Max	14	12.76	7.29	11	13.01	8.88	25	12.87	7.85	0.851	(-5.7 – 5.76)
Peak	13	8.61	5.73	11	8.34	5.66	24	8.49	5.58	0.865	(-4.2 – 4.38)
Mean40%	14	7.85	4.84	10	8.22	4.98	24	8.00	4.79	0.977	(-4.17 – 3.35)
Mean30%	14	6.71	4.33	11	6.68	4.49	25	6.70	4.31	0.893	(-3.11 – 3.17)
MeanMan	14	4.08	2.36	11	3.70	1.88	25	3.91	2.13	0.687	(-1.29 – 2.16)
SUL(g/mL)	**N**	**Moy**	**σ**	**N**	**Moy**	**σ**	**N**	**Moy**	**σ**	**p**	**IC95%**
Max	14	9.03	4.57	11	8.89	5.28	25	8.97	4.79	0.767	(-3.67 – 4.36)
Peak	13	6.00	3.45	11	5.79	3.75	24	5.90	3.51	0.776	(-2.55 – 2.97)
Mean40%	14	5.48	2.97	10	5.63	3.03	24	5.54	2.93	0.977	(-2.64 – 2.41)
Mean30%	14	4.81	2.76	11	4.58	2.79	25	4.71	2.72	0.743	(-2.17 – 2.48)
MeanMan	14	2.84	1.45	11	2.57	1.17	25	2.72	1.32	0.647	(-0.8 – 1.32)
Texture 1st order	**N**	**Moy**	**σ**	**N**	**Moy**	**σ**	**N**	**Moy**	**σ**	**p**	**IC95%**
T40%											
TGL	12	43.28	57.32	10	29.56	25.08	22	37.04	45.16	0.923	(-19.7 – 27.48)
Volume (mL)	12	4.34	2.84	10	4.05	2.99	22	4.21	2.84	0.819	(-2.3 – 2.89)
T40% Ring										0.877	(-0.95 – 1.17)
SUV Mean	13	2.24	0.98	10	2.31	1.49	23	2.27	1.20	0.784	(-3.61 – 3.82)
SUV Max	13	7.29	4.63	10	7.94	5.53	23	7.57	4.93	0.709	(-21.24 – 14.54)
TGL	13	29.58	24.97	10	30.72	21.91	23	30.07	23.17	0.632	(-7.14 – 4.43)
Volume (mL)	13	12.03	5.93	10	13.38	7.44	23	12.62	6.50	0.877	(-0.95 – 1.17)
Texture 2nd order	**N**	**Moy**	**σ**	**N**	**Moy**	**σ**	**N**	**Moy**	**σ**	**p**	**IC95%**
T40%											
Homogeneity	9	0.32	0.13	8	0.31	0.12	17	0.31	0.12	0.815	(-0.11 – 0.11)
Entropy log10	9	2.32	0.48	8	2.31	0.36	17	2.32	0.42	0.987	(-0.44 – 0.45)
GLRLM SRE	9	0.94	0.05	8	0.95	0.04	17	0.95	0.04	0.563	(-0.02 – 0.04)
GLRLM LRE	9	1.33	0.41	8	1.27	0.26	17	1.30	0.34	0.596	(-0.18 – 0.16)
GLZLM LGZE	9	0.01	0.02	8	0.01	0.01	17	0.01	0.01	0.963	(0 – 0)
GLZLM HGZE	9	1074.09	1345.79	8	1006.78	1101.81	17	1042.42	1199.12	0.888	(-970 – 989)
T40% Ring											
Homogeneity	13	0.45	0.14	10	0.47	0.15	23	0.46	0.14	0.799	(-0.14 – 0.11)
Entropy log10	13	1.97	0.52	10	1.96	0.53	23	1.97	0.51	0.969	(-0.45 – 0.47)
GLRLM SRE	13	0.90	0.06	10	0.88	0.08	23	0.89	0.07	0.556	(-0.04 – 0.08)
GLRLM LRE	13	1.77	0.60	10	1.96	0.78	23	1.85	0.67	0.535	(-0.67 – 0.34)
GLZLM LGZE	13	0.04	0.03	10	0.05	0.06	23	0.04	0.04	0.975	(-0.03 – 0.02)
GLZLM HGZE	13	166.69	141.20	10	191.39	183.21	23	177.43	157.36	0.784	(-101.2 – 100)

Table XII: Results of conventional and texture analysis of PET0: Grade 1 of Chevallier versus other patients

Finally, we used Kruskal Wallis test for studying the differences between 3 Chevallier groups.

Results of this complementary analysis are reported in following table.

	Grade 1			Grade 2			Grade 3			Total			Stat
Visual analysis	**N**		**%**	**N**		**%**	**N**		**%**	**N**		**%**	
0	0		0	0		0	0		0	0		0	
1	0		0	0		0	0		0	0		0	
2	1		4	2		8	1		4	4		16	
3	13		52	2		8	6		24	21		81	
Total	***14***		***56***	***4***		***16***	***7***		***28***	***25***		***100***	
SUV (g/mL)	**N**	**Moy**	**σ**	**N**	**Moy**	**σ**	**N**	**Moy**	**σ**	**N**	**Moy**	**σ**	**p**
Max	14	12.76	7.29	4	10.88	9.57	7	14.23	8.99	25	12.87	7.85	0.851
Peak	13	8.61	5.73	4	7.36	8.05	7	8.90	4.47	24	8.49	5.58	0.865
Mean40%	14	7.85	4.84	3	7.90	6.71	7	8.35	4.71	24	8.00	4.79	0.977
Mean30%	14	6.71	4.33	4	5.60	5.54	7	7.30	4.14	25	6.70	4.31	0.893
MeanMan	14	4.08	2.36	4	3.47	2.56	7	3.84	1.59	25	3.91	2.13	0.687
SUL(g/mL)	**N**	**Moy**	**σ**	**N**	**Moy**	**σ**	**N**	**Moy**	**σ**	**N**	**Moy**	**σ**	**p**
Max	14	9.03	4.57	4	7.99	6.93	7	9.41	4.64	25	8.97	4.79	0.767
Peak	13	6.00	3.45	4	5.47	5.82	7	5.97	2.53	24	5.90	3.51	0.776
Mean40%	14	5.48	2.97	3	5.82	4.82	7	5.55	2.45	24	5.54	2.93	0.977
Mean30%	14	4.81	2.76	4	4.11	4.01	7	4.85	2.17	25	4.71	2.72	0.743
MeanMan	14	2.84	1.45	4	2.56	1.85	7	2.57	0.76	25	2.72	1.32	0.647
Texture 1st order	**N**	**Moy**	**σ**	**N**	**Moy**	**σ**	**N**	**Moy**	**σ**	**N**	**Moy**		**p**
T40%													
TGL	12	43.28	57.32	4	26.23	34.98	6	31.77	19.57	22	37.04	45.16	-
Volume (mL)	12	4.34	2.84	4	3.85	3.99	6	4.18	2.54	22	4.21	2.84	-
T40% Ring													
SUV Mean	13	2.24	0.98	4	1.86	1.15	6	2.61	1.71	23	2.27	1.20	-
SUV Max	13	7.29	4.63	4	6.35	5.45	6	8.99	5.82	23	7.57	4.93	-
TGL	13	29.58	24.97	4	25.05	26.86	6	34.51	19.70	23	30.07	23.17	-
Volume (mL)	13	12.03	5.93	4	12.86	10.62	6	13.73	5.61	23	12.62	6.50	-
Texture 2nd order	**N**	**Moy**	**σ**	**N**	**Moy**	**σ**	**N**	**Moy**	**σ**	**N**	**Moy**	**σ**	**p**
T40%													
Homogeneity	9	0.32	0.13	2	0.36	0.23	6	0.29	0.09	17	0.31	0.12	-
Entropy log10	9	2.32	0.48	2	2.27	0.74	6	2.33	0.27	17	2.32	0.42	-
GLRLM SRE	9	0.94	0.05	2	0.93	0.07	6	0.96	0.02	17	0.95	0.04	-
GLRLM LRE	9	1.33	0.41	2	1.47	0.53	6	1.20	0.13	17	1.30	0.34	-
GLZLM LGZE	9	0.01	0.02	2	0.02	0.02	6	0.00	0.00	17	0.01	0.01	-
GLZLM HGZE	9	1074.09	1345.79	2	1277.05	1729.51	6	916.69	1030.72	17	1042.42	1199.12	-
T40% Ring													
Homogeneity	13	0.45	0.14	4	0,54	0.18	6	0.42	0.13	23	0.46	0.14	-
Entropy log10	13	1.97	0.52	4	1,73	0.62	6	2.12	0.46	23	1.97	0.51	-
GLRLM SRE	13	0.90	0.06	4	0,84	0.11	6	0.91	0.04	23	0.89	0.07	-
GLRLM LRE	13	1.77	0.60	4	2,36	1.10	6	1.69	0.40	23	1.85	0.67	-
GLZLM LGZE	13	0.04	0.03	4	0,09	0.08	6	0.02	0.02	23	0.04	0.04	-
GLZLM HGZE	13	166.69	141.20	4	140,23	154.85	6	225.51	206.25	23	177.43	157.36	-

Table XIII : Results of conventional and texture analysis of PET0: Grade 1 versus Grade 2 versus Grade 3 of Chevallier

15 Patients showed suspicious lymph node uptakes on PET0, corresponding to 23 measured lesions.

Numbers and quantitative parameters of lymph nodes, according to their clinical and pathological status, are reported in the next page table.

	pN0		pN1		Total PET N+	
Numbers	**N**	**%**	**N**	**%**	**N**	**%**
Patients						
cN0	2	13	1	07	9	60
cN1	4	27	1	07	6	40
Total	*6*	*40*	*2*	*13*	*15*	*100*
Lesions						
cN0	4	19	1	05	13	57
cN1	6	29	1	05	10	43
Total	*10*	*48*	*2*	*10*	*23*	*100*
Quantitative values	**N**	**Moy (g/mL)**	**N**	**Moy (g/mL)**	**N**	**Moy (g/mL)**
SUV Max						
cN0	4	3.15	1	11.18	13	4.84
cN1	6	10.80	1	39.76	10	11.36
Total	*10*	*7.74*	*2*	*25.47*	*23*	*7.67*
SUV Peak						
cN0	4	1.52	1	7.62	13	2.62
cN1	4	4.12	1	23.20	8	5.64
Total	*8*	*2.82*	*2*	*15.41*	*21*	*3.77*
SUL Max						
cN0	4	2.48	1	8.61	13	3.45
cN1	6	8.02	1	23.57	10	7.87
Total	*10*	*5.80*	*2*	*16.09*	*23*	*5.37*
SUL Peak						
cN0	4	1.20	1	5.87	13	1.92
cN1	4	2.88	1	13.75	8	3.73
Total	*8*	*2.04*	*2*	*9.81*	*21*	*2.61*

Table XIV: Results of PET0 nodal analysis

Annexe 7: Numbers and average values of interim PET conventional and textural analysis, depending on pathological results

We performed a complementary statistical analysis on our interim PET population, between patients corresponding to Grade of 1 of Chevallier and the group composed by Grade 2 and Grade 3.

Exact test of Fisher was used for qualitative variables and Wilcoxon Mann Whitney test for quantitative ones. Results of these analysis are reported on three following tables.

	Grade 1			Grades 2+3			Total			Statistics	
Visual analysis	**N**	**%**		**N**	**%**		**N**	**%**		**p**	
CR	2	9.5		1	4.8		3	14,3			
PR	11	52.4		6	28.6		17	81,0			
SD	1	4.8		0	0		1	0,0		***1***	
PD	0	0.0		0	0		0	0,0			
Total	***14***	***66.7***		***7***	***33.3***		***21***	***100***			
ΔSUV	**N**	**Moy (%)**	**σ**	**N**	**Moy (%)**	**σ**	**N**	**Moy (%)**	**σ**	**p**	**IC95%**
Max	13	-52	19	6	-61	14	19	-55	18	0.578	(-0.27 – 0.16)
Peak	12	-52	15	6	-58	19	18	-54	16	0.639	(-0.24 – 0.16)
Mean40%	11	-54	16	5	-62	16	16	-57	16	0.678	(-0.24 – 0.17)
Mean30%	9	-53	17	4	-58	12	13	-55	15	0.843	(-0.21 – 0.26)
MeanMan	15	-48	24	6	-49	16	21	-49	21	0.977	(-0.25 – 0.26)
ΔSUL	**N**	**Moy (%)**	**σ**	**N**	**Moy (%)**	**σ**	**N**	**Moy (%)**	**σ**	**p**	**IC95%**
Max	13	-53	19	6	-61	14	19	-55	18	0.544	(-0.27 – 0.15)
Peak	12	-52	16	6	-59	19	18	-54	16	0.574	(-0.25 – 0.15)
Mean40%	11	-54	17	5	-63	16	16	-57	16	0.613	(-0.25 – 0.16)
Mean30%	9	-54	19	4	-59	12	13	-55	17	0.897	(-0.23 – 0.26)
MeanMan	14	-40	19	6	-50	16	20	-43	18	0.437	(-0.29 – 0.13)
PERCIST	**N**	**%**		**N**	**%**		**N**	**%**		**p**	
CMR	1	05		0	00		1	05			
PMR	1	05		7	35		8	40			
SMD	10	50		0	00		10	50		***1***	
PD	1	05		0	00		1	05			
Total	***13***	***65***		***7***	***35***		***20***	***100***			

Table XV: Results of conventional analysis of PET1: Grade 1 of Chevallier versus other patients

	Grade 1			Grade 2+3			Total			Statistics	
ΔTexture 1st ordre	**N**	**Moy (%)**	**σ**	**N**	**Moy (%)**	**σ**	**N**	**Moy (%)**	**σ**	**p**	**IC95%**
T40%											
TGL	7	-54.72	21.35	5	-71.68	15.48	12	-65.89	20.25	0.429	(-16.88 – 36.73)
Volume	7	-52.04	24.26	5	-39.62	30.67	12	07.06	107.83	0.626	(-38.77 – 338.43)
T40% Ring											
SUV Mean	9	-39.87	21.22	6	-52.29	9.92	15	-44.84	18.22	0.207	(-7.78 – 32.62)
SUV Max	9	-52.16	21.36	6	-58.99	8.81	15	-54.89	17.33	0.955	(-9.11 – 13.2)
TGL	9	-18.21	57.82	6	-34.78	77.86	15	-24.84	64.39	0.272	(-18.03 – 87.52)
Volume	9	42.84	97.74	6	33.87	163.80	15	39.25	122.73	0.388	(-30.16 – 168.73)
T40% Repro											
SUV Mean	4	-68.17	16.11	6	-71.91	12.78	10	-70.42	13.45	0.692	(-17.27 – 24.77)
SUV Max	4	-52.98	30.35	6	-62.73	11.93	10	-58.83	20.28	0.914	(-19.66 – 51.14)
SUVPeak 0,5mL	3	-53.93	30.63	3	-68.08	22.56	6	-61.00	25.28	0.554	(-46.83 – 75.14)
SUVPeak 1mL	3	-56.28	28.85	2	-56.85	4.97	5	-56.50	20.56	0.981	(-68.37 – 69.52)
TGL	4	-65.72	14.62	6	-67.87	15.05	10	-67.01	14.08	0.829	(-20.01 – 24.31)
Volume	4	16.09	40.73	6	13.87	20.39	10	14.76	28.02	0.911	(-41.98 – 46.43)
T40% Ring Repro											
SUV Mean	5	-49.25	13.37	6	-54.52	9.84	11	-52.12	11.29	0.470	(-10.54 – 21.08)
SUV Max	5	-30.55	32.78	6	-48.18	21.14	11	-40.16	27.17	0.308	(-19.26 – 54.54)
TGL	5	-50.01	13.86	6	-56.16	8.94	11	-53.36	11.27	0.396	(-9.45 – 21.75)
Volume	5	-1.13	9.83	6	-3.22	3.98	11	-02.27	06.91	0.644	(-7.77 – 11.94)

Table XVI: Results of first order textural analysis of PET1: Grade 1 of Chevallier versus other patients

	Grade 1			Grade 2+3			Total			Statistics	
ΔTexture 2nd ordre	**N**	**Moy (%)**	**σ**	**N**	**Moy (%)**	**σ**	**N**	**Moy (%)**	**σ**	**p**	**IC95%**
T40%											
Homogeneity	6	54.87	40.35	4	38.10	8.76	10	48.16	31.70	0.365	(-25.5 – 59.04)
Entropy log10	6	-27.06	18.01	4	-21.39	9.59	10	-24.80	14.81	0.762	(-33.84 – 13.99)
GLRLM SRE	6	-10.49	17.29	4	-4.59	3.39	10	-08.13	13.39	0.914	(-38.3 – 5.6)
GLRLM LRE	6	101.82	205.99	4	27.25	24.13	10	71.99	158.90	0.990	(-42.64 – 478.19)
GLZLM LGZE	6	485.97	331.88	4	485.42	349.97	10	485.75	319.40	0.998	(-503.71 – 504.82)
GLZLM HGZE	6	-72.98	24.81	4	-76.12	7.55	10	-74.24	10.07	0.610	(-18.38 – 45.28)
T40% Ring											
Homogeneity	9	39.94	21.60	6	52.96	21.80	15	45.15	21.91	0.275	(-37.7 – 11.66)
Entropy log10	9	-33.13	17.38	6	-34.63	11.34	15	-33.73	14.80	0.856	(-15.97 – 18.97)
GLRLM SRE	9	-15.77	16.66	6	-15.91	12.90	15	-15.83	14.77	0.776	(-13.2 – 13.02)
GLRLM LRE	9	111.76	170.85	6	110.59	108.90	15	111.29	144.62	0.607	(-89.69 – 52.31)
GLZLM LGZE	9	387.45	304.50	6	625.79	497.94	15	482.78	395.15	0.268	(-682.87 – 206.18)
GLZLM HGZE	9	-64.46	24.93	6	-74.02	9.35	15	-68.28	20.25	0.776	(-7.96 – 26.17)
T40% Repro											
Homogeneity	4	64.89	40.92	6	86.25	51.21	10	77.70	62.88	0.628	(-119.08 – 76.37)
Entropy log10	4	-27.10	24.04	6	-23.24	-24.91	10	-24.79	17.85	0.759	(-31.87 – 24.15)
GLRLM SRE	4	-15.20	21.04	6	-9.06	-9.01	10	-11.52	13.40	0.762	(-37.78 – 11.14)
GLRLM LRE	4	130.06	201.59	6	58.80	51.45	10	87.30	127.34	0.990	(-85.26 – 381.33)
GLZLM LGZE	4	1784.68	1258.12	6	2990.82	1864.49	10	2508.36	2141.76	0.476	(-5079.07 – 1833.9)
GLZLM HGZE	4	-79.91	16.20	6	-84.56	-81.34	10	-82.70	11.75	0.571	(-13.5 – 22.8)
T40% Ring Repro											
Homogeneity	5	53.44	24.29	6	67.91	31.99	11	61.33	28.37	0.428	(-53.94 – 25.01)
Entropy log10	5	-30.97	15.22	6	-35.31	10.92	11	-33.34	12.55	0.595	(-13.47 – 22.16)
GLRLM SRE	5	-21.91	16.84	6	-20.17	8.02	11	-20.96	12.10	0.826	(-19.16 – 15.68)
GLRLM LRE	5	147.74	113.66	6	127.59	50.86	11	136.75	81.06	0.704	(-95.9 – 136.2)
GLZLM LGZE	5	392.22	358.36	6	620.15	568.94	11	516.55	476.84	0.459	(-894.65 – 438.79)
GLZLM HGZE	5	-51.14	35.44	6	-68.39	17.53	11	-60.55	27.15	0.319	(-19.73 – 54.23)

Table XVII: Results of second order textural analysis of PET1: Grade 1 of Chevallier versus other patients

Finally, we used Kruskal Wallis test for studying the differences between 3 Chevallier groups. Results of this complementary analysis concerning conventional evaluation are reported in the following table.

	Grade 1			Grade 2			Grade 3			Total			Stat
Visual Analysis	**N**		**%**	**N**		**%**	**N**		**%**	**N**		**%**	**p**
CR	2		9,5	1		4,8	0		0,0	3		14,3	
PR	11		52,4	2		9 ,5	4		19,0	17		81,0	
SD	1		4,8	0		0,0	0		0,0	1		0,0	***1***
PD	0		0,0	0		0,0	0		0,0	0		0,0	
Total	***14***		***66,7***	***3***		***14,3***	***4***		***19,0***	***21***		***100***	
ΔSUV	**N**	**Moy (%)**	**σ**	**N**	**Moy (%)**	**σ**	**N**	**Moy (%)**	**σ**	**N**	**Moy (%)**	**σ**	**p**
Max	13	-52	19	2	-63	13	4	-60	16	19	-55	18	0.640
Peak	12	-52	15	2	-59	35	4	-57	14	18	-54	16	0.782
Mean40%	11	-54	16	1	-73	-	4	-60	18	16	-57	16	0.535
Mean30%	9	-53	17	1	-74	-	3	-53	07	13	-55	15	0.474
MeanMan	15	-48	24	2	-50	35	4	-48	07	21	-49	21	0.993
ΔSUL	**N**	**Moy (%)**	**σ**	**N**	**Moy (%)**	**σ**	**N**	**Moy (%)**	**σ**	**N**	**Moy (%)**	**σ**	**P**
Max	13	-53	19	2	-63	13	4	-60	16	19	-55	18	0.636
Peak	12	-52	16	2	-59	35	4	-58	14	18	-54	16	0.742
Mean40%	11	-54	17	1	-73	-	4	-60	18	16	-57	16	0.514
Mean30%	9	-54	19	1	-74	-	3	-54	09	13	-55	17	0.543
MeanMan	14	-40	19	2	-50	35	4	-49	07	20	-43	18	0.566
PERCIST	**N**		**%**	**N**		**%**	**N**		**%**	**N**		**%**	**p**
CMR	1		5	0		0	0		0	1		5	
PMR	1		5	3		15	4		20	8		40	
SMD	10		50	0		0	0		0	10		50	***1***
PD	1		5	0		0	0		0	1		5	
Total	***13***		***65***	***3***		***15***	***4***		***20***	***20***		***100***	

Table XVIII: Results of conventional analysis of PET1: Grade 1 versus Grade 2 versus Grade 3 of Chevallier

Only one patient of textural evaluation was classed Grade 2 of Chevallier, so we did not perform a comparison between 3 groups. Average textural values of different groups are reported in two tables, on next page.

	Grade 1			Grade 2			Grade 3			Total		
ΔTexture 1st ordre	**N**	**Moy (%)**	**σ**	**N**	**Moy (%)**	**σ**	**N**	**Moy (%)**	**σ**	**N**	**Moy (%)**	**σ**
T40%												
TGL	7	-54.72	21.35	1	-97.30	-	4	-65.27	6.78	12	-65.89	20.25
Volume	7	-52.04	24.26	1	-89.40	-	4	-27.17	14.89	12	07.06	107.83
T40% Ring												
SUV Mean	9	-39.87	21.22	1	-69.51	-	5	-48.85	5.83	15	-44.84	18.22
SUV Max	9	-52.16	21.36	1	-70.21	-	5	-56.75	7.70	15	-54.89	17.33
TGL	9	-18.21	57.82	1	-91.82	-	5	-23.37	81.25	15	-24.84	64.39
Volume	9	42.84	97.74	1	-73.18	-	5	55.28	173.49	15	39.25	122.73
T40% Repro												
SUV Mean	4	-68.17	16.11	1	-90.45	-	5	-68.21	10.05	10	-70.42	13.45
SUV Max	4	-52.98	30.35	1	-71.35	-	5	-61.01	12.47	10	-58.83	20.28
SUVPeak 0,5mL	3	-53.93	30.63	1	-93.67	-	2	-55.28	5.96	6	-61.00	25.28
SUVPeak 1mL	3	-56.28	28.85	0	-	-	2	-56.85	4.97	5	-56.50	20.56
TGL	4	-65.72	14.62	1	-90.48	-	5	-63.34	11.38	10	-67.01	14.08
Volume	4	16.09	40.73	1	0	-	5	16.64	21.50	10	14.76	28.02
T40% Ring Repro												
SUV Mean	5	-49.25	13.37	1	-72.62	-	5	-50.89	4.76	11	-52.12	11.29
SUV Max	5	-30.55	32.78	1	-74.20	-	5	-42.98	18.85	11	-40.16	27.17
TGL	5	-50.01	13.86	1	-72.67	-	5	-52.86	4.25	11	-53.36	11.27
Volume	5	-1.13	9.83	0	-	-	5	-3.86	4.09	11	-02.27	06.91

Table XIX: Results of first order textural analysis of PET1: Grade 1 versus Grade 2 versus Grade 3 of Chevallier

	Grade 1			Grade 2			Grade 3			Total		
ΔTexture 2nd ordre	**N**	**Moy (%)**	**σ**	**N**	**Moy (%)**	**σ**	**N**	**Moy (%)**	**σ**	**N**	**Moy (%)**	**σ**
T40%												
Homogeneity	6	54.87	40.35	0	-	-	4	38.10	8.76	10	48.16	31.70
Entropy log10	6	-27.06	18.01	0	-	-	4	-21.39	9.59	10	-24.80	14.81
GLRLM SRE	6	-10.49	17.29	0	-	-	4	-4.59	3.39	10	-08.13	13.39
GLRLM LRE	6	101.82	205.99	0	-	-	4	27.25	24.13	10	71.99	158.90
GLZLM LGZE	6	485.97	331.88	0	-	-	4	485.42	349.97	10	485.75	319.40
GLZLM HGZE	6	-72.98	24.81	0	-	-	4	-76.12	7.55	10	-74.24	10.07
T40% Ring												
Homogeneity	9	39.94	21.60	1	93.97	-	5	44.76	9.46	15	45.15	21.91
Entropy log10	9	-33.13	17.38	1	-42.19	-	5	-33.12	11.99	15	-33.73	14.80
GLRLM SRE	9	-15.77	16.66	1	-13.62	-	5	-16.37	14.37	15	-15.83	14.77
GLRLM LRE	9	111.76	170.85	1	87.31	-	5	115.24	121.08	15	111.29	144.62
GLZLM LGZE	9	387.45	304.50	1	490.91	-	5	652.77	551.79	15	482.78	395.15
GLZLM HGZE	9	-64.46	24.93	1	-82.45	-	5	-72.34	9.38	15	-68.28	20.25
T40% Repro												
Homogeneity	4	64.89	40.92	1	219.90	-	5	59.52	44.80	10	77.70	62.88
Entropy log10	4	-27.10	24.04	1	-44.80	-	5	-18.93	11.63	10	-24.79	17.85
GLRLM SRE	4	-15.20	21.04	1	-19.53	-	5	-6.97	4.08	10	-11.52	13.40
GLRLM LRE	4	130.06	201.59	1	143.12	-	5	41.93	28.72	10	87.30	127.34
GLZLM LGZE	4	1784.68	1258.12	1	7549.25	-	5	2079.14	1423.83	10	2508.36	2141.76
GLZLM HGZE	4	-79.91	16.20	1	-94.80	-	5	-82.51	8.32	10	-82.70	11.75
T40% Ring Repro												
Homogeneity	5	53.44	24.29	1	125.40	-	5	56.41	16.96	11	61.33	28.37
Entropy log10	5	-30.97	15.22	1	-49.61	-	5	-32.45	9.37	11	-33.34	12.55
GLRLM SRE	5	-21.91	16.84	1	-24.82	-	5	-19.24	8.60	11	-20.96	12.10
GLRLM LRE	5	147.74	113.66	1	167.91	-	5	119.53	52.40	11	136.75	81.06
GLZLM LGZE	5	392.22	358.36	1	1384.85	-	5	467.21	478.73	11	516.55	476.84
GLZLM HGZE	5	-51.14	35.44	1	-89.78	-	5	-64.11	15.71	11	-60.55	27.15

Table XX: Results of second order analysis of PET1: Grade 1 versus Grade 2 versus Grade 3 of Chevallier

13 patients with suspicious nodal uptakes on PET0 were evaluated on PET1. Among them, five was in CR (39%), seven was in PR (54%) and one remains stable (8%), according to visual assessment.

20 suspicious nodal uptakes on PET0 was evaluated on PET1. 10 out of them was in CR (50%), nine (45%) was in PR and 1 (5%) remains stable, on visual assessment.

None visual PD was visualized on PET1.

Qualitative parameters of lymph nodes assessment on PET1, according to their clinical and pathological status, are reported in the following table.

	pN0		pN1		Total PET N+	
Numbers	**N**	**%**	**N**	**%**	**N**	**%**
Patients						
cN0						
CR	2	15	0	00	4	31
PR	1	08	0	00	3	23
cN1						
CR	1	08	0	00	1	08
PR	3	23	0	00	4	31
SD	0	00	1	08	1	08
Total	7	54	1	08	13	100
Lesions						
cN0						
CR	4	20	0	00	6	30
PR	1	05	0	00	4	20
cN1						
CR	2	10	0	00	4	20
PR	4	20	0	00	5	25
SD	0	00	1	05	1	05
Total	11	55	1	05	20	100

Table XXI: Results of PET1 nodal analysis - qualitative description

Variations of conventionnal quantitative parameters of nodal uptakes on PET1, according to their clinical staging and pathological results, are reported in the next page table.

	pN0		pN1		Total PET N+	
Quantitative values	**N**	**ΔMoy (%)**	**N**	**ΔMoy (%)**	**N**	**ΔMoy (%)**
SUV Max						
cN0						
CR	1	-25.68%	0	-	2	-49.71%
PR	1	-81.57%	0	-	4	-44.72%
cN1				-		
CR	0	-	0	-	0	-
PR	4	-71.65%	0	-	5	-67.95%
SD	0	-	1	-24.04	1	-24.04%
SUV Peak						
cN0						
CR	1	-27.43%	0	-	2	-45.17%
PR	1	-81.91%	0	-	4	-45.19%
cN1				-		
CR	0	-	0	-	0	-
PR	2	-62.71%	0	-	3	-59.55%
SD	0	-	1	-16.25	1	-16.25%
SUL Max						
cN0						
CR	1	-25.00%	0	-	2	-49.46%
PR	1	-81.60%	0	-	4	-44.94%
cN1				-		
CR	0	-	0	-	0	-
PR	4	-72.61%	0	-	5	-68.61%
SD	0	-	1	-22.70	1	-22.70%
SUL Peak						
cN0						
CR	1	-26.37%	0	-	2	-44.48%
PR	1	-82.06%	0	-	4	-45.10%
cN1				-		
CR	0	-	0	-	0	-
PR	2	-63.05%	0	-	3	-59.65%
SD	0	-	1	-14.76	1	-14.76%

Table XXII: Results of PET1 nodal analysis - quantitative description

SERMENT D'HIPPOCRATE – VERSION LONGUE

Au moment d'être admis(e) à exercer la médecine, je promets et je jure d'être fidèle aux lois de l'honneur et de la probité.

Mon premier souci sera de rétablir, de préserver ou de promouvoir la santé dans tous ses éléments, physiques et mentaux, individuels et sociaux.

Je respecterai toutes les personnes, leur autonomie et leur volonté, sans aucune discrimination selon leur état ou leurs convictions. J'interviendrai pour les protéger si elles sont affaiblies, vulnérables ou menacées dans leur intégrité ou leur dignité. Même sous la contrainte, je ne ferai pas usage de mes connaissances contre les lois de l'humanité.

J'informerai les patients des décisions envisagées, de leurs raisons et de leurs conséquences.
Je ne tromperai jamais leur confiance et n'exploiterai pas le pouvoir hérité des circonstances pour forcer les consciences.

Je donnerai mes soins à l'indigent et à quiconque me les demandera. Je ne me laisserai pas influencer par la soif du gain ou la recherche de la gloire.

Admis(e) dans l'intimité des personnes, je tairai les secrets qui me seront confiés.
Reçu(e) à l'intérieur des maisons, je respecterai les secrets des foyers et ma conduite ne servira pas à corrompre les mœurs.
Je ferai tout pour soulager les souffrances. Je ne prolongerai pas abusivement les agonies. Je ne provoquerai jamais la mort délibérément.

Je préserverai l'indépendance nécessaire à l'accomplissement de ma mission. Je n'entreprendrai rien qui dépasse mes compétences. Je les entretiendrai et les perfectionnerai pour assurer au mieux les services qui me seront demandés.

J'apporterai mon aide à mes confrères ainsi qu'à leurs familles dans l'adversité.

Que les hommes et mes confrères m'accordent leur estime si je suis fidèle à mes promesses ; que je sois déshonoré(e) et méprisé(e) si j'y manque.

Nom, Prénom Signature

SERMENT D'HIPPOCRATE – VERSION COURTE

En présence des Maîtres de cette FACULTE et de mes chers CONDISCIPLES, je promets et je jure d'être fidèle aux lois de l'Honneur et de la Probité dans l'exercice de la Médecine.

Je donnerai mes soins gratuits à l'indigent et je n'exigerai jamais un salaire au-dessus de mon travail. Admis dans l'intérieur des maisons, mes yeux ne verront pas ce qui s'y passe, ma langue taira les secrets qui me seront confiés et mon état ne servira pas à corrompre les mœurs ni à favoriser le crime.

Respectueux et reconnaissant envers mes MAÎTRES, je rendrai à leurs enfants l'instruction que j'ai reçue de leurs pères.

Que les HOMMES m'accordent leur estime si je suis fidèle à mes promesses. Que je sois couvert d'OPPROBRE et méprisé de mes confrères si j'y manque.

Nom, Prénom Signature

Prédiction de la réponse thérapeutique précoce par TEP au ^{18}FDG dans le cancer du sein HER2+ : Approche conventionnelle et analyse texturale en situation néoadjuvante.

Résumé :

Contexte : La TEP au 18F-fluorodéoxyglucose (^{18}FDG) est recommandée dans le bilan d'extension initial des néoplasies mammaires localement avancées. Plusieurs études ont montré la valeur pronostique du bilan d'extension par cette modalité, mais sa valeur prédictive de réponse complète anatomopathologique reste incertaine.
Objectif : Le but de cette étude est d'évaluer la valeur prédictive de la fixation tumorale initiale et de l'évaluation thérapeutique précoce par TEP au ^{18}FDG, par étude conventionnelle et analyse de texture, chez les patientes présentant une néoplasie mammaire HER2+.
Méthode : Les patientes étudiées étaient celles de l'évaluation intermédiaire de l'étude prospective et multicentrique française NeoTOP. Toutes présentaient un cancer du sein HER2+ et étaient éligibles à une chimiothérapie néoadjuvante. Elles ont bénéficié d'une TEP au ^{18}FDG initialement et après la première cure de traitement néoadjuvant. Les examens étaient étudiés par méthode conventionnelle et par analyse texturale. Les réponses anatomopathologiques complètes correspondaient aux grades 1 et 2 de la classification de Chevallier des pièces opératoires.
Résultats : Les résultats anatomopathologiques étaient disponibles pour 27 patientes, d'âge moyen 53 ans. Le SUV max initial moyen des tumeurs était de 12,87 (s=7,85) g/mL, avec une diminution moyenne de 56% après une cure, sans différence entre les patients répondeurs et non-répondeurs (p>0,5). Il n'a pas été retrouvé de différence significative entre les groupes lorsque la fixation tumorale était mesurée par les autres méthodes visuelles ou quantitatives conventionnelles. Les valeurs initiales et la variation des paramètres de texture entre les deux examens, concernant à la fois la zone tumorale et la zone péritumorale, ne différaient pas entre les groupes.
Conclusion : Le bilan d'extension et l'évaluation thérapeutique précoce par TEP au ^{18}FDG pour les néoplasies mammaires HER2 + ne sont pas prédictifs de la réponse anatomopathologique après traitement néoadjuvant, que ce soit par étude conventionnelle ou en analyse de texture.

Mots-clés:

- HER2+
- ^{18}FDG PET/CT
- Texture Analysis
- Neoadjuvant treatment
- Pathological Complete Response
- NeoTOP